EIC synergies: nuclear imaging at the EIC/UPCs

Wenbin Zhao

Lawrence Berkeley National Laboratory

University of California, Berkeley

Collaborators: Heikki Mäntysaari, Farid Salazar, Björn Schenke, and Chun Shen

June 3 – 7, 2024 Boston, USA

Diffraction in optics

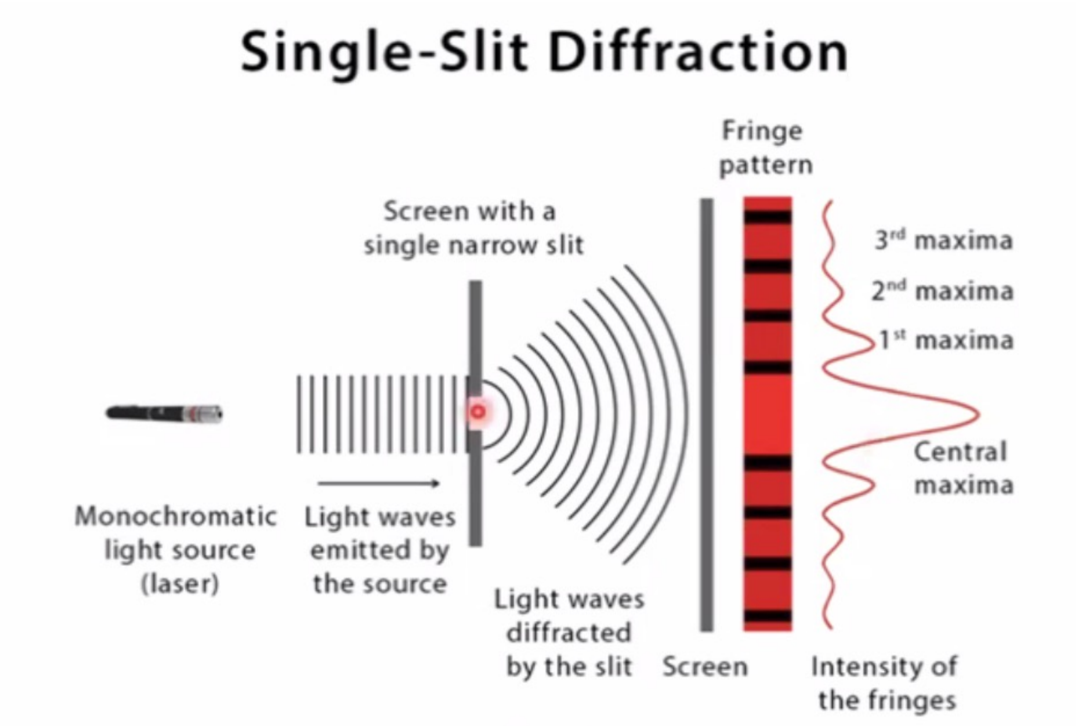

Taken from J. D. Brandemburg's slide.

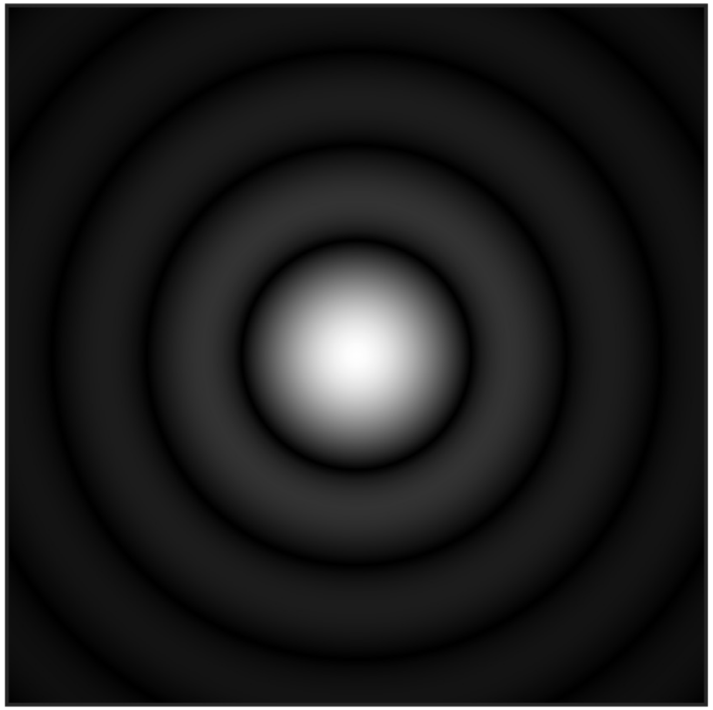

Taken from Wiki

- Diffraction: in momentum-space the positions of the minima and maxima of diffraction pattern are determined solely by the target size R.

Yuri V. Kovchegov, QUANTUM CHROMODYNAMICS A T HIGH ENERGY.

Diffraction in the High Energy Collisions

Diffractive vector meson production

High energy factorization:

1. $\gamma^* \to q\bar{q}$ splitting,
   wave function $\Psi^\gamma(r, Q^2, z)$
2. $q\bar{q}$ dipole scatters elastically
3. $q\bar{q} \to J/\Psi$, wave function $\Psi^V(r, Q^2, z)$

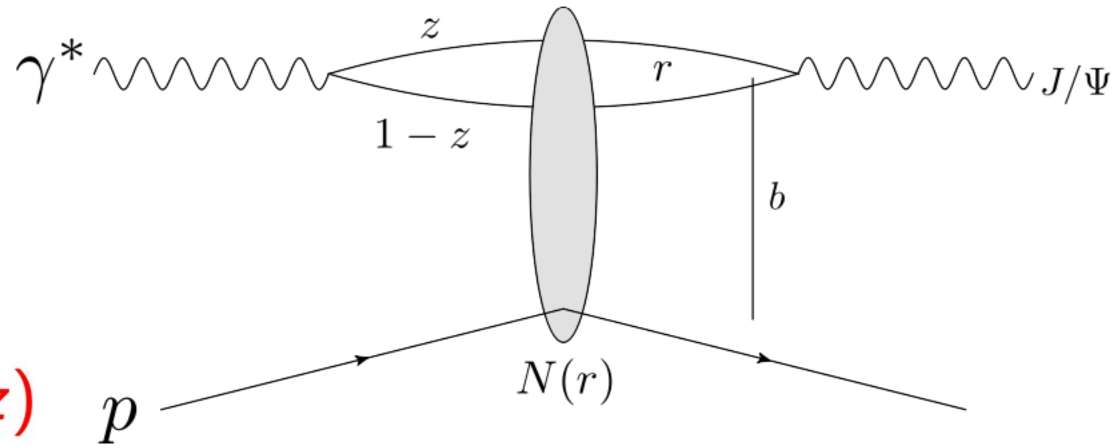

Diffractive scattering amplitude (~ Fourier transform of the spatial structure of target).

$$\mathcal{A}^{\gamma^* p \to Vp} \sim \int \mathrm{d}^2 b \mathrm{d}z \mathrm{d}^2 r \Psi^{\gamma *} \Psi^V (r, z, Q^2) \mathbf{e}^{-\mathbf{i}\mathbf{b}\cdot\boldsymbol{\Delta}} N(r, x, b)$$

Impact parameter, b, is the Fourier conjugate of the momentum transfer, $\Delta \approx \sqrt{-t}$

IP-Sat: $N(\mathbf{r}_T, \mathbf{b}_T, x) = 1 - \exp\left(-\mathbf{r}_T{}^2 F(\mathbf{r}_T, x) T_p(\mathbf{b}_T)\right)$, **accesses the spatial structure ($T_{p/A}$)**

$F(\mathbf{r}_T, x) = \dfrac{\pi^2}{2N_c} \alpha_s(\mu^2) x g(x, \mu^2)$. $xg(x, \mu^2)$, gluon density at x and scale μ^2 ($\mu^2 \sim \mu_0^2 + 1/r_T^2$).

In this work, we describe the dipole target interactions by CGC model. (See details in back-up)

Miettinen, Pumplin, PRD 18, 1978; Caldwell, Kowalski, 0909.1254; Mäntysaari, Schenke, 1603.04349; Mäntysaari, 2001.10705

Coherent and incoherent processes

- **Coherent** $\sigma_{\text{coherent}} \sim |\langle \mathcal{A} \rangle_\Omega|^2$

Target stays intact, (|initial state> = |final state>)
Probes the average shape of the target.

- **Incoherent** $\sigma_{\text{incoherent}} \sim \langle |\mathcal{A}|^2 \rangle_\Omega - |\langle \mathcal{A} \rangle_\Omega|^2$

Target breaks apart, (|initial state> ≠ |final state>)

Probes the variance of event-by-event initial state fluctuations in target structure.

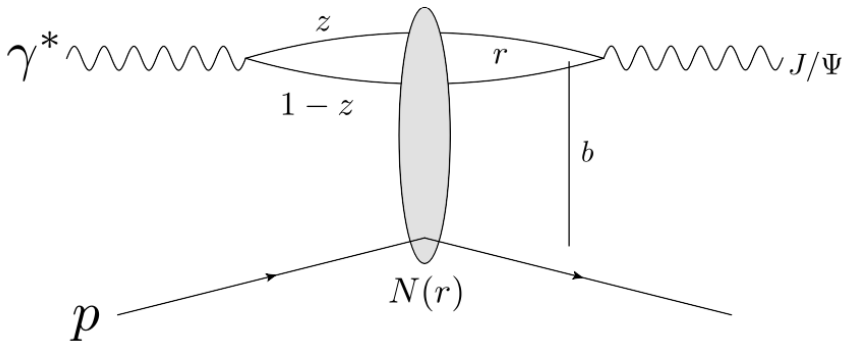

Miettinen, Pumplin, PRD 18, 1978; Caldwell, Kowalski, 0909.1254; Mäntysaari, Schenke, 1603.04349; Mäntysaari, 2001.10705

Accessing nuclear deformation at small x

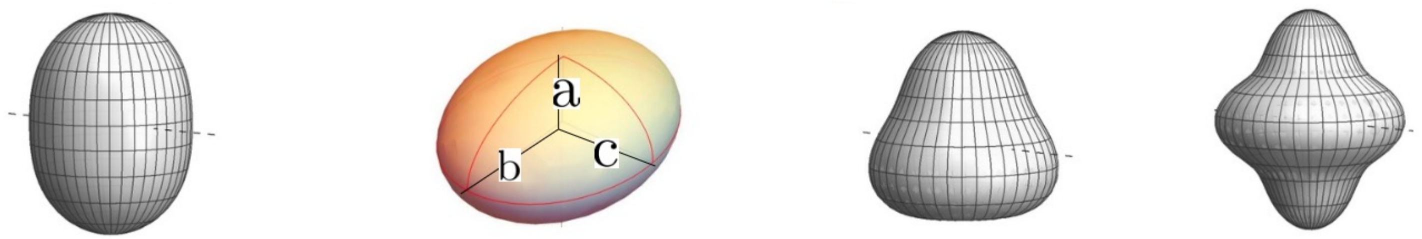

Nuclear structure

Generalized Woods-Saxon profile

$$\rho(r,\Theta,\Phi) \propto \frac{1}{1+\exp\left(\left[r-R(\Theta,\Phi)\right]/a\right)}\ , \quad R(\Theta,\Phi) = R_0\left[1+\underline{\beta_2}\left(\cos\underline{\gamma} Y_{20}(\Theta)+\sin\gamma Y_{22}(\Theta,\Phi)\right)+\underline{\beta_3}Y_{30}(\Theta)+\underline{\beta_4}Y_{40}(\Theta)\right]$$

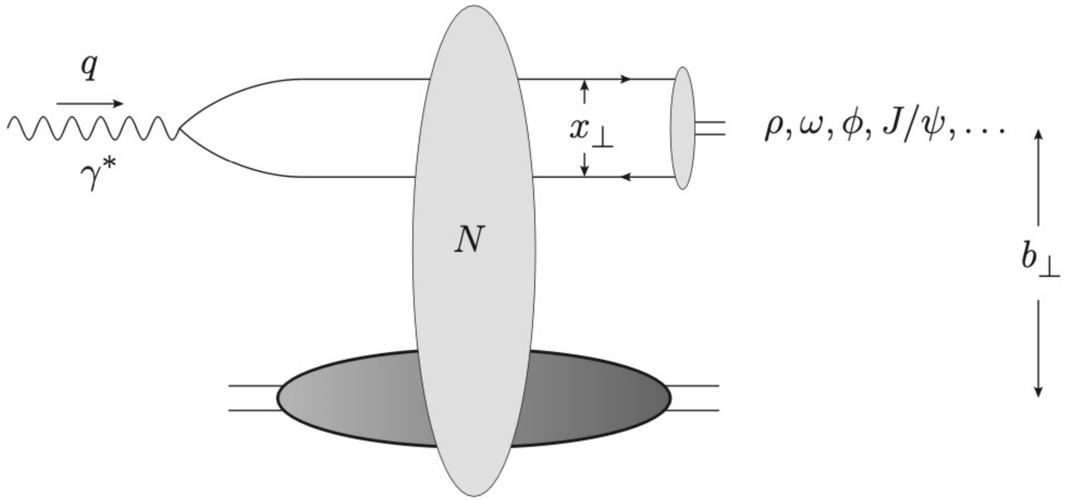

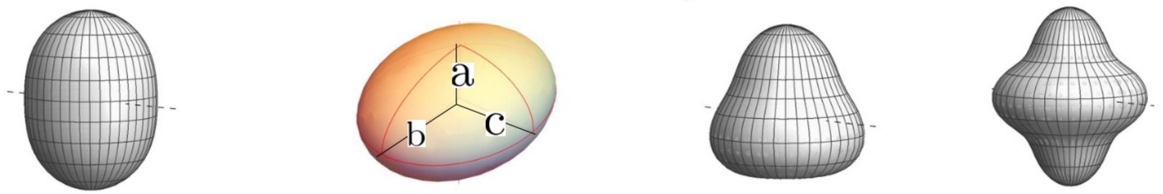

Taken from Giuliano's slide

- Different deformation parameters control the geometric deformation at different length scale.
- Probe the nuclear geometric deformation by the diffractive process.

γ^* + U → J/ψ + U*

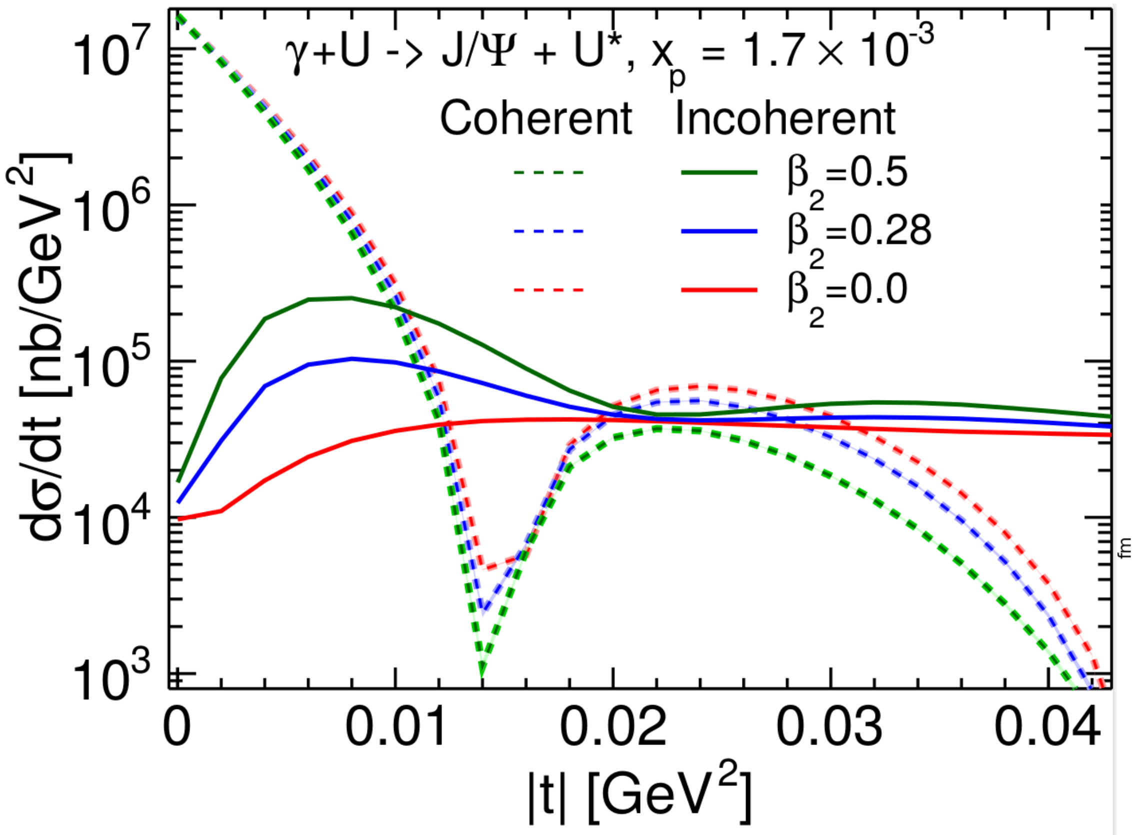

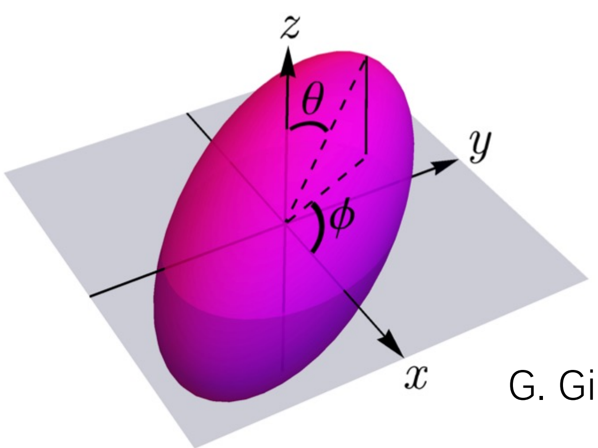

G. Giacalone, arXiv: 2004.14463

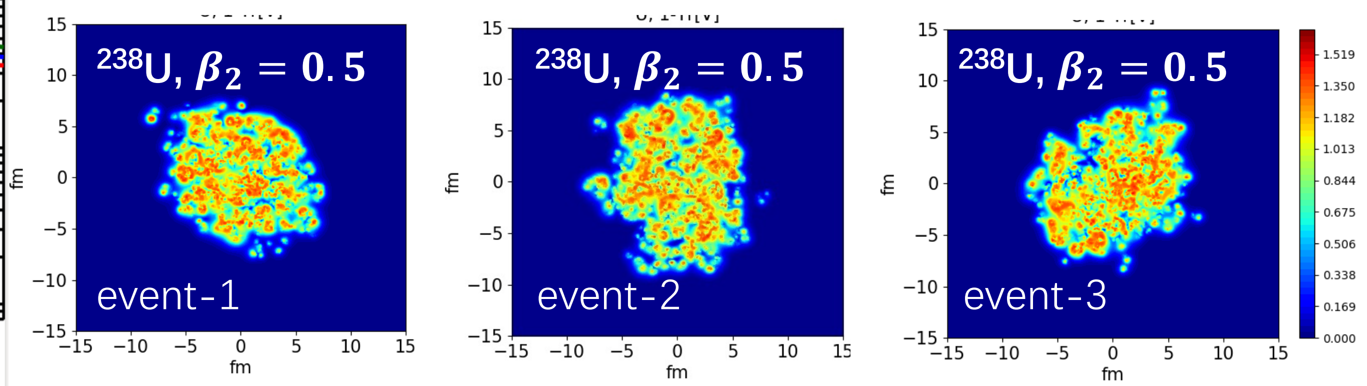

- Large β_2 enhances the fluctuations of the configurations projected onto x-y plane.
- β_2 enhances incoherent cross section at small |t|.

H.Mantysaari, B.Schenke, C. Shen and W. Zhao, PhysRevLett.131.062301.

Multi-scale imaging: Nuclear deformations

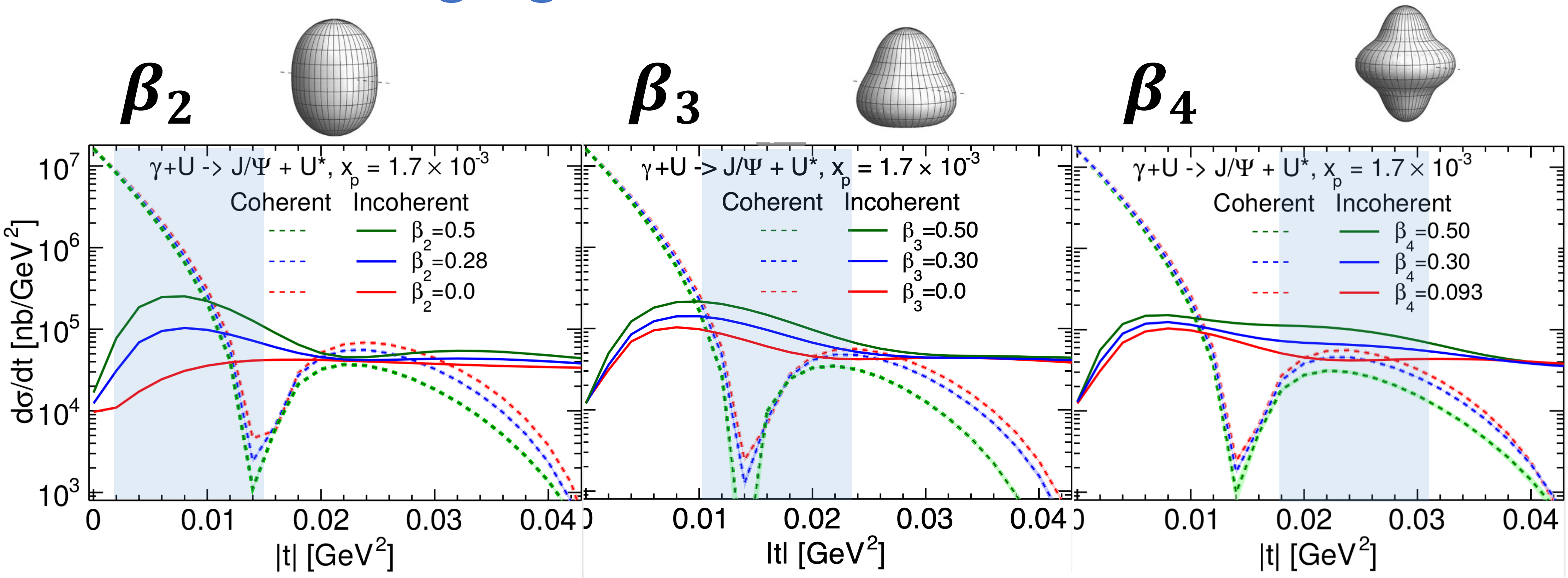

- β_2 , β_3 and β_4 manifest themselves at different |t| regions (different length scales).

H.Mantysaari, B.Schenke, C. Shen and W. Zhao, PhysRevLett.131.062301.

Multi-scale imaging : "See" sub-nucleonic structures

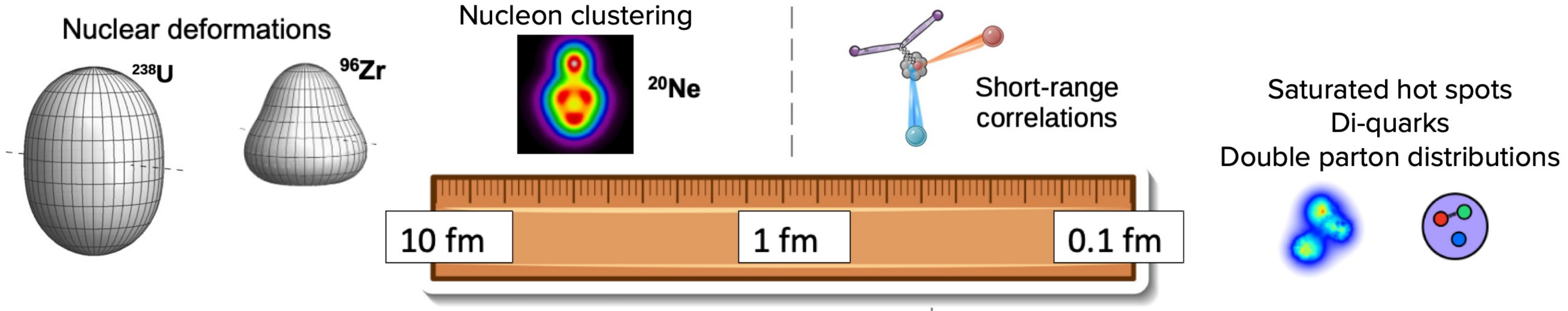

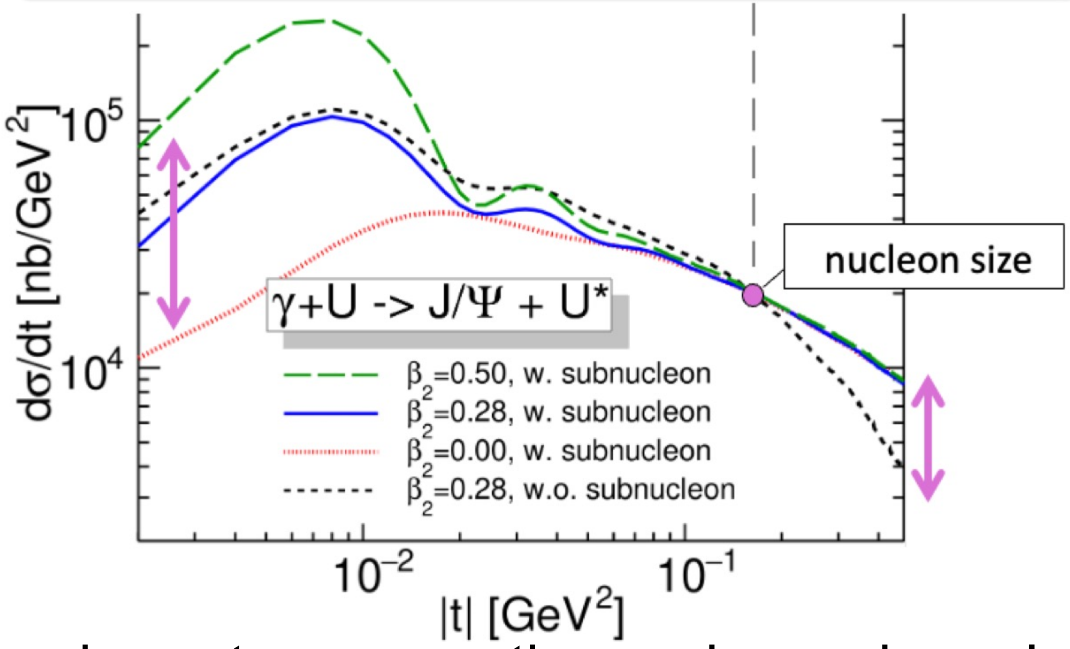

The transverse momentum transfer sets the length scale we probe

Illustration by G. Giacalone

- High |t| region of γ^* + A incoherent cross section probes sub-nucleon structures.

H.Mantysaari, B.Schenke, C. Shen and W. Zhao, Phys. Lett. B 833 (2022), 137348.
H.Mantysaari, B.Schenke, C. Shen and W. Zhao, PhysRevLett.131.062301.

Probing Nuclear Deformations in UPCs

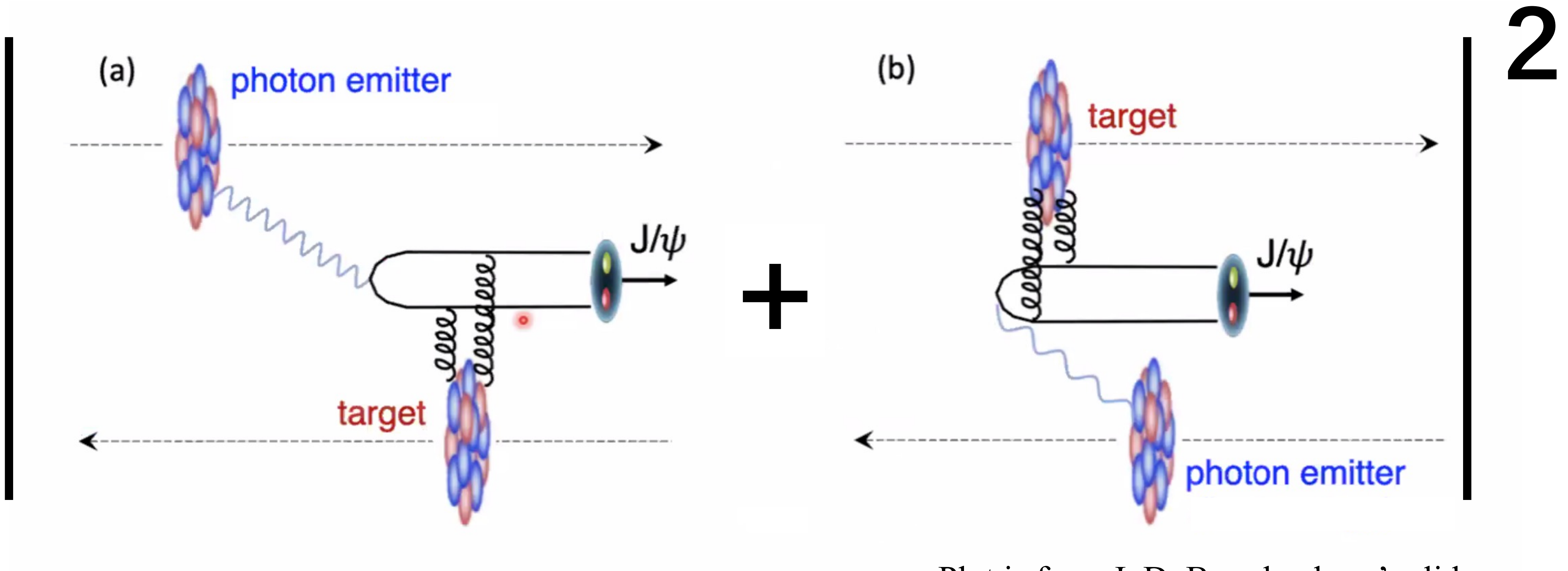

Plot is from J. D. Brandemburg's slide.

Interference Measurement in Au+Au and U+U

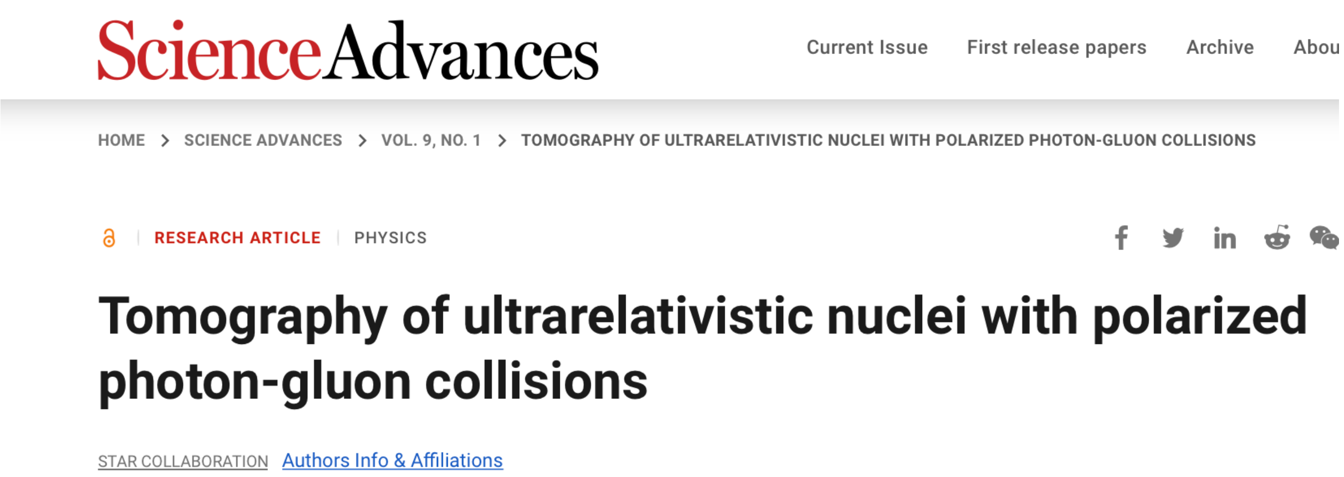
ScienceAdvances

Current Issue First release papers Archive Abou

HOME > SCIENCE ADVANCES > VOL. 9, NO. 1 > TOMOGRAPHY OF ULTRARELATIVISTIC NUCLEI WITH POLARIZED PHOTON-GLUON COLLISIONS

RESEARCH ARTICLE | PHYSICS

Tomography of ultrarelativistic nuclei with polarized photon-gluon collisions

STAR COLLABORATION Authors Info & Affiliations

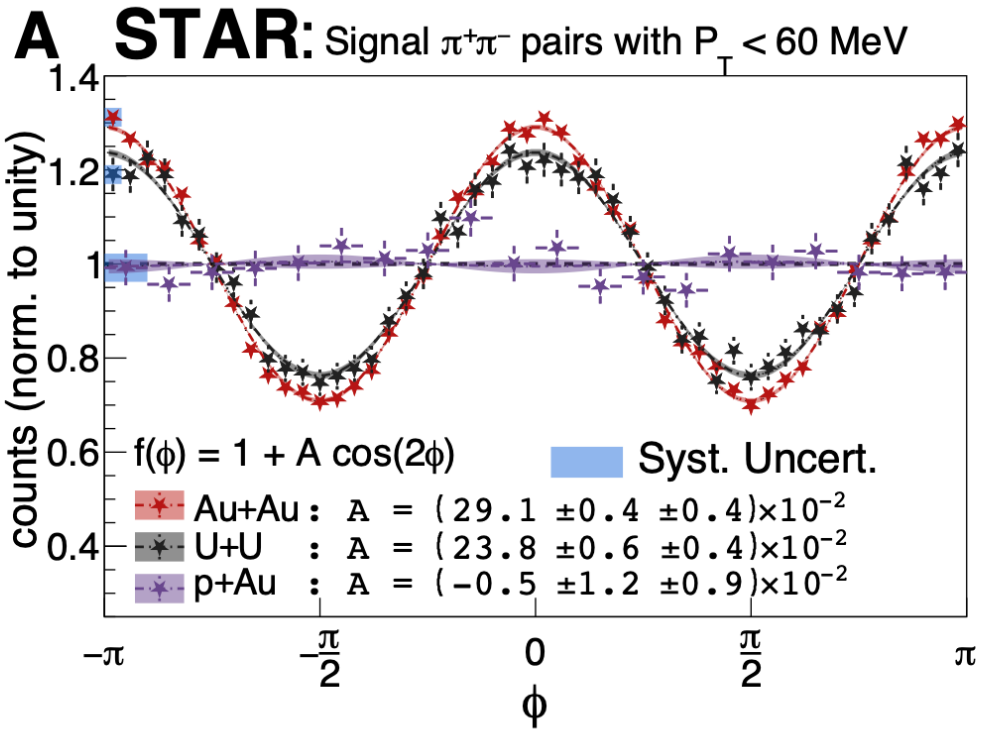

- Beautiful interference pattern observed in UPCs by STAR people.
- The interference effect is sensitive to the nuclear geometry.

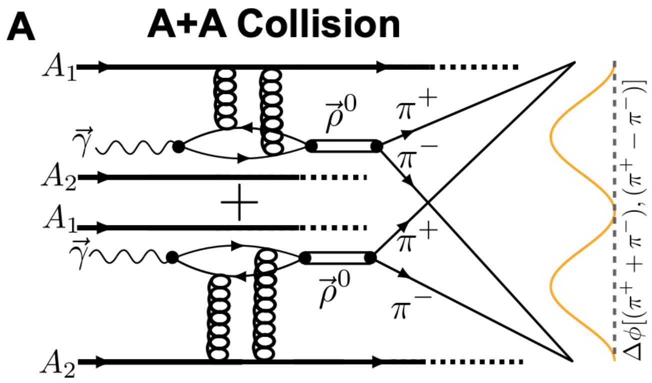

STAR Sci. Adv. 9 (2023) no.1, eabq3903.

Double-slit interference in UPCs

$$\frac{d\sigma^{\rho\to\pi^+\pi^-}}{d^2\mathbf{P}_\perp dq_\perp dy_1 dy_2} = \frac{1}{2(2\pi)^3}\frac{P_\perp^2}{(Q^2-M_V^2)^2+M_V^2\Gamma^2} f^2_{\rho\pi\pi}\left\{\int d\phi_{\mathbf{q}_\perp} B_\perp dB_\perp \langle \mathcal{M}^i(y,\mathbf{q}_\perp,\mathbf{B}_\perp)\mathcal{M}^{\dagger,j}(y,\mathbf{q}_\perp,\mathbf{B}_\perp)\rangle_\Omega P_\perp^i P_\perp^j \Theta(|\mathbf{B}_\perp|-B_{\min,\Omega})\right\}$$

- The amplitude:

$$\mathcal{M}^i(x_1,x_2,\boldsymbol{q}_\perp,\boldsymbol{B}_\perp) = \int d^2\boldsymbol{b}_\perp e^{-i\boldsymbol{q}_\perp\cdot\boldsymbol{b}_\perp}\left[\widetilde{A}(\boldsymbol{b}_\perp)_{A_1,x_1}\widetilde{\mathcal{F}}^i_{A_2}(x_2,\boldsymbol{b}_\perp-\boldsymbol{B}_\perp)+\widetilde{A}(\boldsymbol{b}_\perp-\boldsymbol{B}_\perp)_{A_2,x_2}\widetilde{\mathcal{F}}^i_{A_1}(x_1,\boldsymbol{b}_\perp)\right]$$

- Subscripts A_1 and A_2 refer to the colliding nuclei. x_1 and x_2: Bjorken x, b: impact parameter of the photon-nucleus collision, B: impact parameter of the nucleus-nucleus collision.
- The function $\widetilde{\mathcal{F}}^j_A($ is the photon flux.
- Diffractive scattering amplitude

$$A^{\gamma^* p\to Vp} \sim \int d^2b\,dz\,d^2r\,\Psi^{\gamma*}\Psi^V(r,z,Q^2)e^{-ib\cdot\Delta}N(r,x,b)$$

H. Xing, C. Zhang, J. Zhou and Y. J. Zhou, JHEP 10(2020), 064.
J. D. Brandenburg, Z. Xu, W. Zha, C. Zhang, J. Zhou and Y. Zhou, PhysRevD.106.074008.
H.Mantysaari, F. Salazar, B.Schenke, C. Shen and W. Zhao, in preparation.

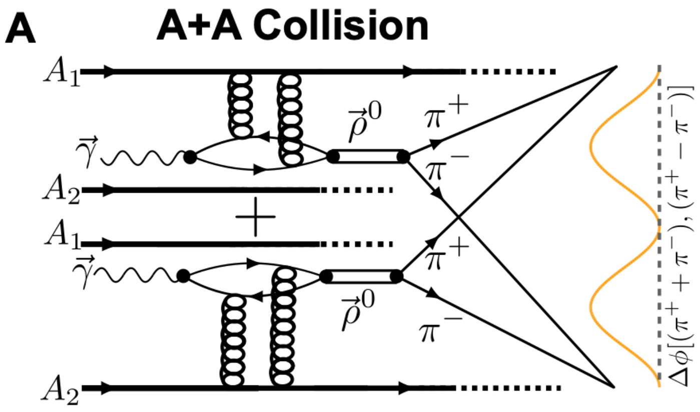

Interference in Au+Au and U+U

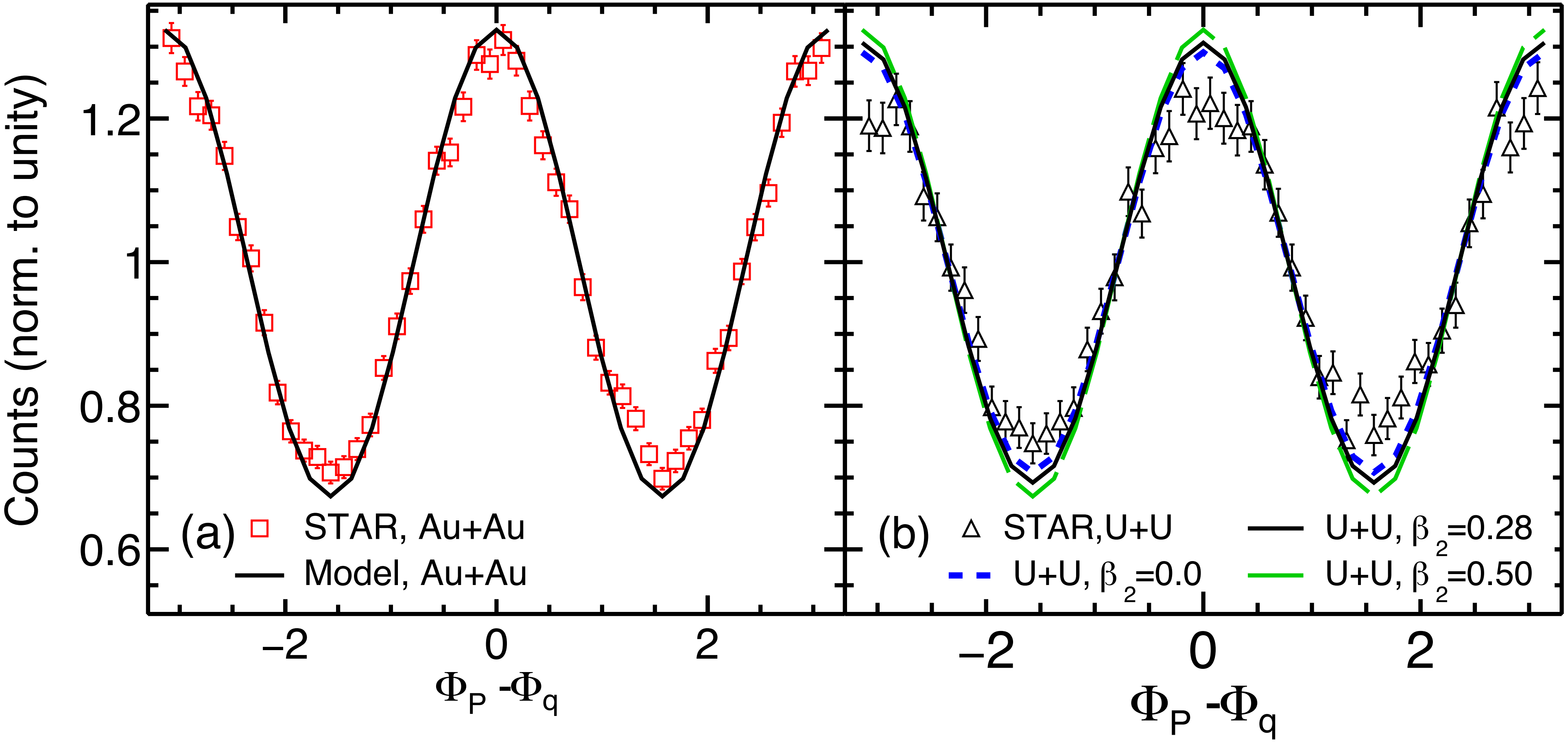

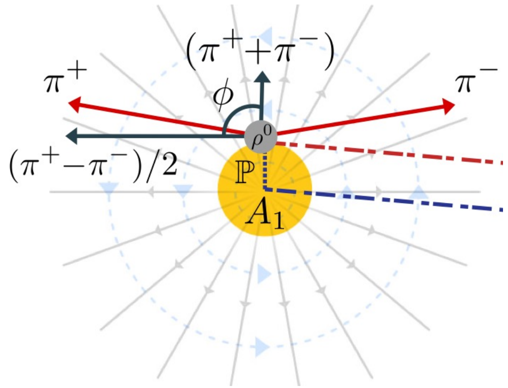

- Our model nicely reproduces the $\cos(2\Delta\Phi)$ modulation.
- In U+U, larger β_2 leads to slightly more pronounced $\cos(2\Delta\Phi)$ modulation.

H.Mantysaari, F. Salazar, B.Schenke, C. Shen and W. Zhao, in preparation.
STAR Sci. Adv. 9 (2023) no.1, eabq3903.

Interference in Au+Au and U+U

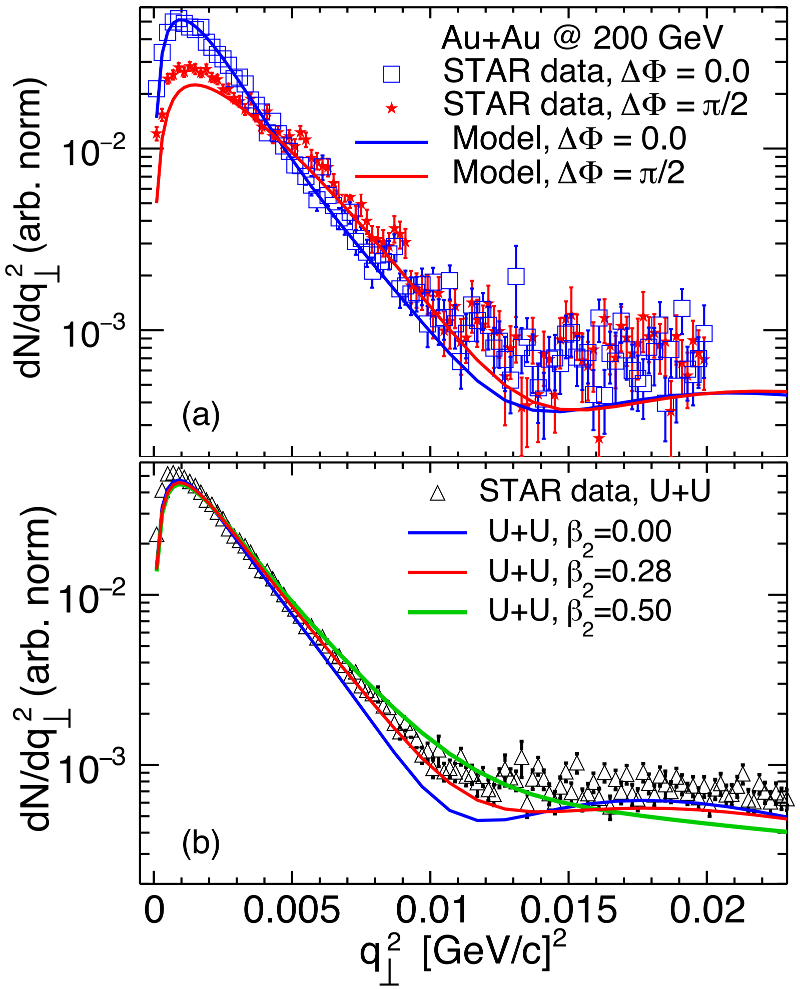

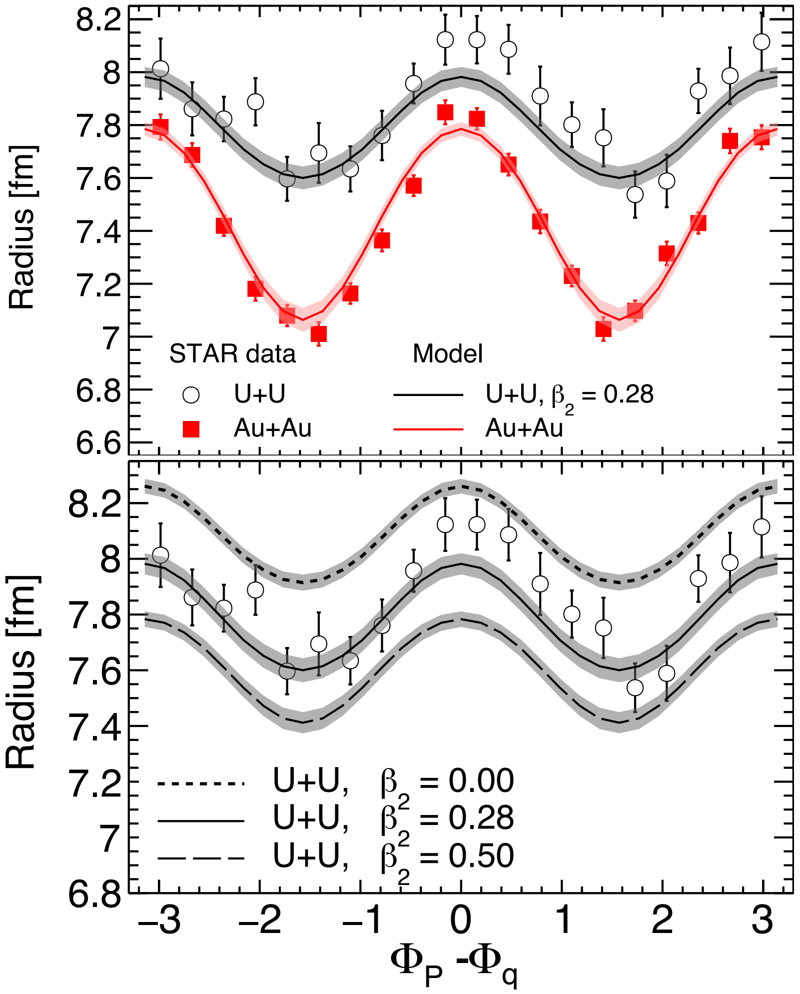

$$\frac{d\sigma^{\gamma^*+A\to VM+A^*}}{dt} \sim e^{-R\,|t|}$$

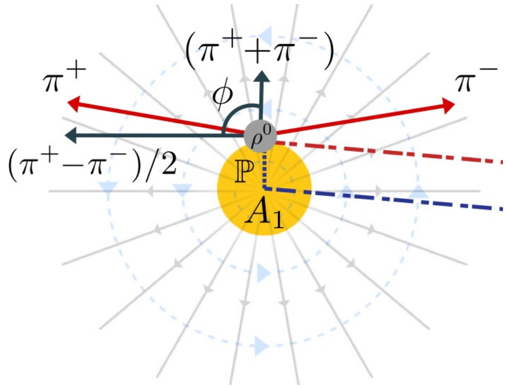

- In U+U, larger β_2 leads to flatter spectra (smaller radius). Larger β_2 has larger incoherent at low $q_\perp^2$, leads to the flatter $dN/dq_\perp^2$. Also the initial photon kT is more important.

H.Mantysaari, F. Salazar, B.Schenke, C. Shen and W. Zhao, in preparation.
STAR Sci. Adv. 9 (2023) no.1, eabq3903.

Probing isobar, Ru/Zr

system	R_0 [fm]	a_0 [fm]	β_2	β_3	β_4
case1 (Ru+Ru)	5.09	0.46	0.16	0.0	0.0
case2 (Ru+Ru)	5.09	0.46	0.16	0.20	0.0
case3 (Ru+Ru)	5.09	0.46	0.06	0.20	0.0
case4 (Ru+Ru)	5.09	0.52	0.06	0.20	0.0
case5 (Zr+Zr)	5.02	0.52	0.06	0.20	0.0

$$R(\Theta,\Phi) = R_0\left[1 + \underline{\beta_2}\left(\cos\gamma Y_{20}(\Theta) + \sin\underline{\gamma} Y_{22}(\Theta,\Phi)\right) + \underline{\beta_3} Y_{30}(\Theta) + \underline{\beta_4} Y_{40}(\Theta)\right]$$

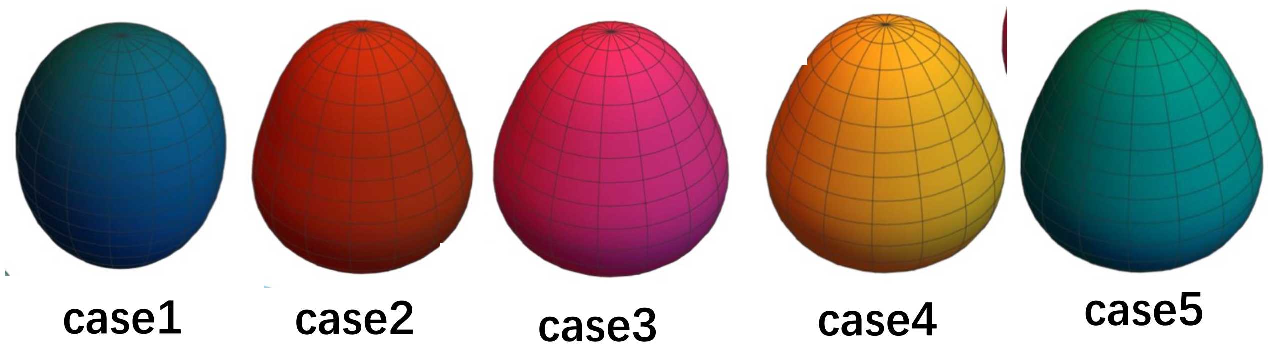

Taken from W. M. Serenone's slide.

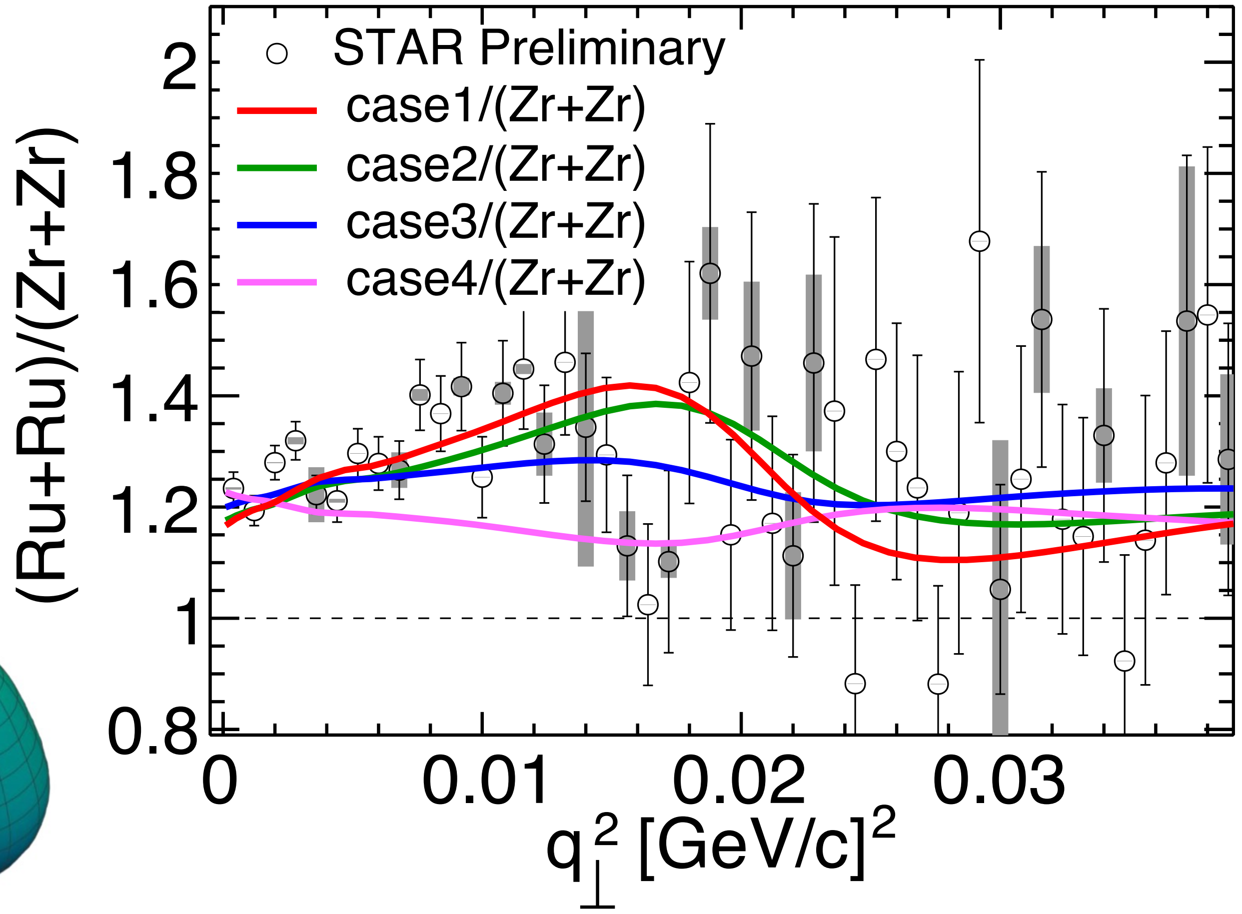

- The vector meson production in isobar UPCs is sensitive to the nuclear structures.
- “By eyes”, the ``full’’ Ru/Zr (case1/case5) is closest to data.

H.Mantysaari, F. Salazar, B.Schenke, C. Shen and W. Zhao, in preparation.

Spatial imaging of polarized deuterons

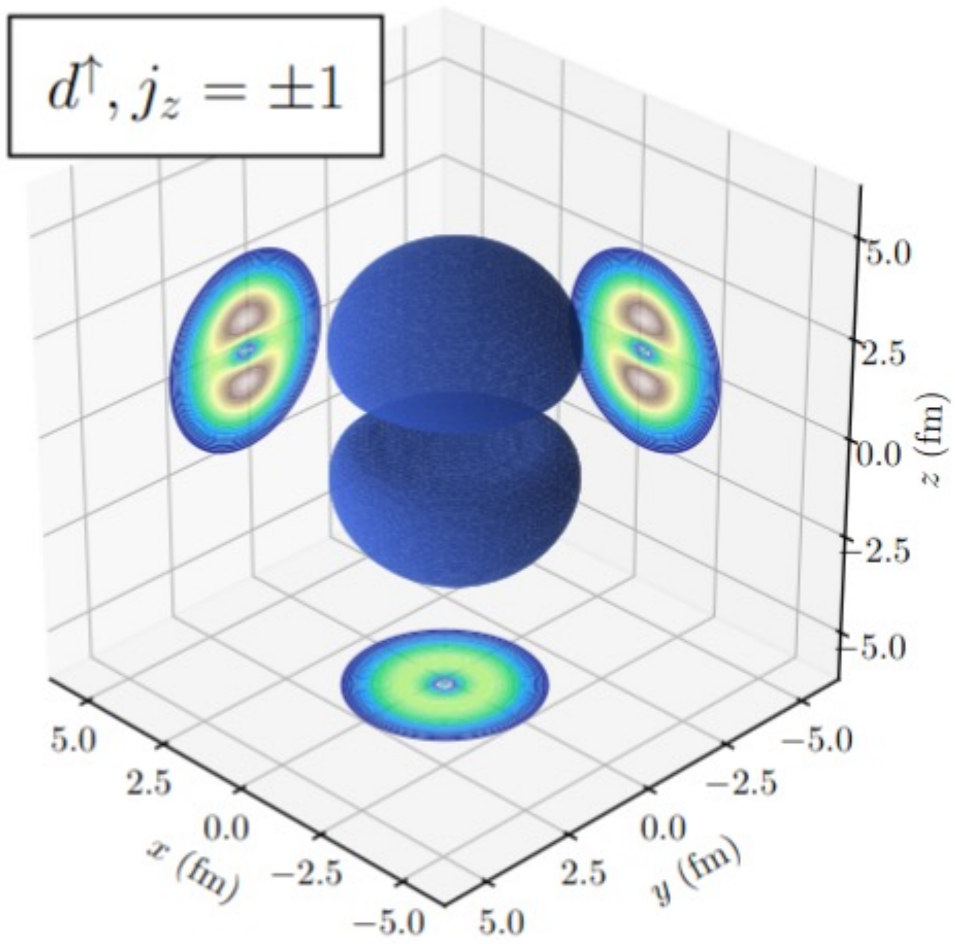

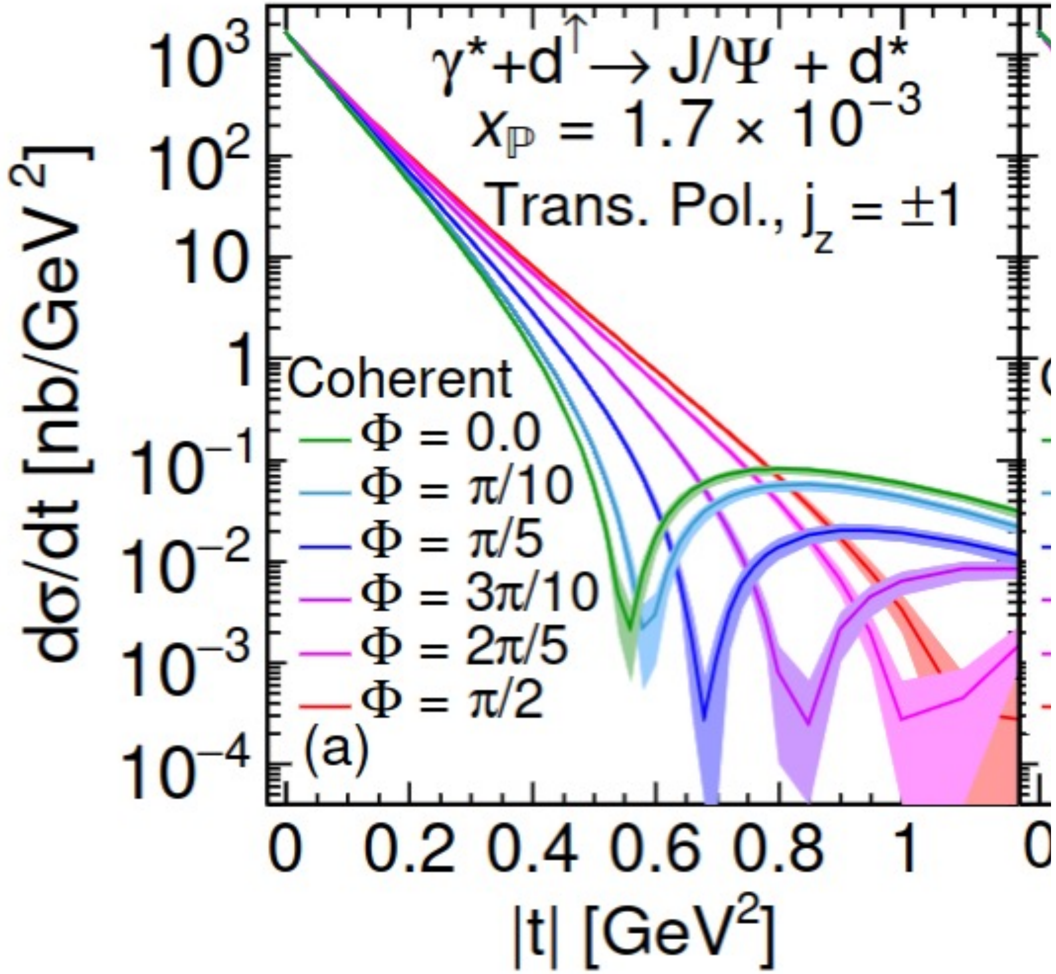

- Angular dependence of the coherent cross section in $e + d^{\uparrow}$ of transverse polarizations.
- Highlight the importance of polarized target in future EIC.

H.Mantysaari, F. Salazar, B.Schenke, C. Shen and W. Zhao, in preparation.

Summary

- Diffractive vector meson production can "see" the nuclear shape and fluctuations at different length scales!
- Vector meson productions in UPCs open up opportunities for investigations the nuclear structures.
- Spatial image of polarized target in the future.

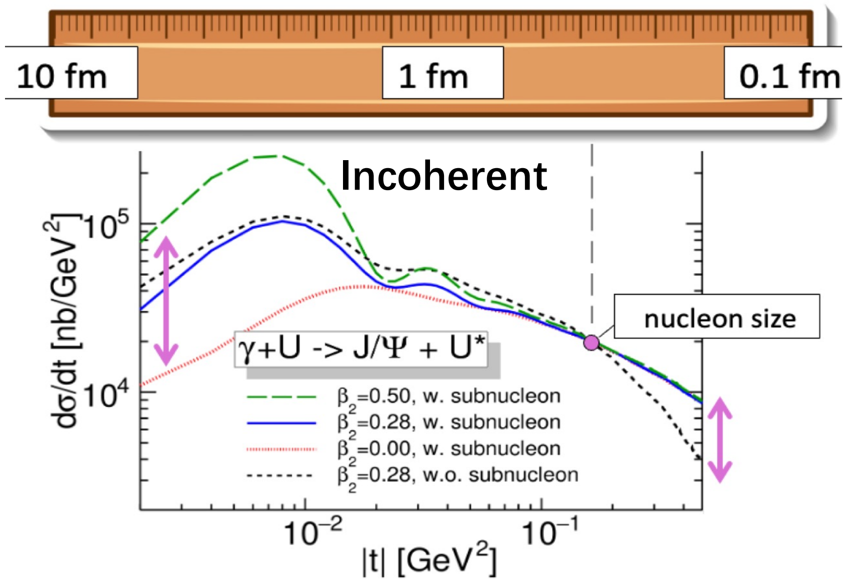

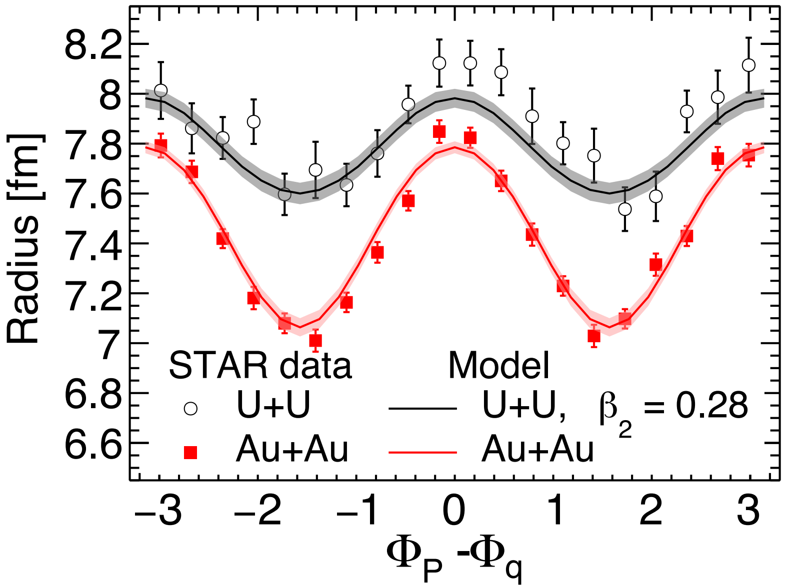

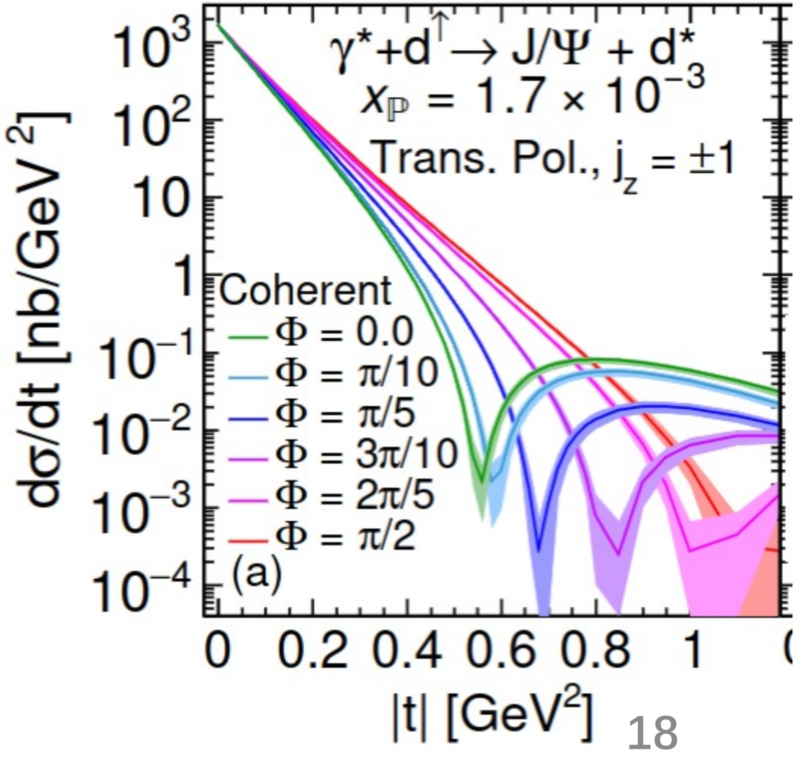

Thanks for Your Attentions!

Back Up

Dipole-target scattering amplitude (CGC)

- The dipole amplitude N can be calculated from Wilson line V(x)

$$N\left(\mathbf{b}=\frac{\mathbf{x}+\mathbf{y}}{2},\mathbf{r}=\mathbf{x}-\mathbf{y},x_{\mathbb{P}}\right)=1-\frac{1}{N_c}\operatorname{Tr}\left(V(\mathbf{x})V^{\dagger}(\mathbf{y})\right)\quad V(\mathbf{x})=P\exp\left(-ig\int dx^{-}\frac{\rho(x^{-},\mathbf{x})}{\boldsymbol{\nabla}^{2}+m^{2}}\right)$$

- Using MV model for Gaussian distribution of color charge ρ:

$$\langle\rho^{a}(\mathbf{b}_{\perp})\rho^{b}(\mathbf{x}_{\perp})\rangle=g^{2}\mu^{2}(x,\mathbf{b}_{\perp})\delta^{ab}\delta^{(2)}(\mathbf{b}_{\perp}-\mathbf{x}_{\perp})$$

Q_s: saturation scale, $Q_s/g^2\mu$ is a free parameter, Q_s is determined from IP-Sat parametrization.

- Or, equivalently, factorize $\mu(x,\mathbf{b}_{\perp})\sim T(\mathbf{b}_{\perp})\mu(x)$

$\boxed{\text{N(r, x, b) accesses to the spatial structure of the target } (T_{p/A}).}$

Schenke , etc.al. PhysRevLett.108.252301 , PhysRevC.86.034908, Mäntysaari, Schenke, 1603.04349;

Posterior Distribution

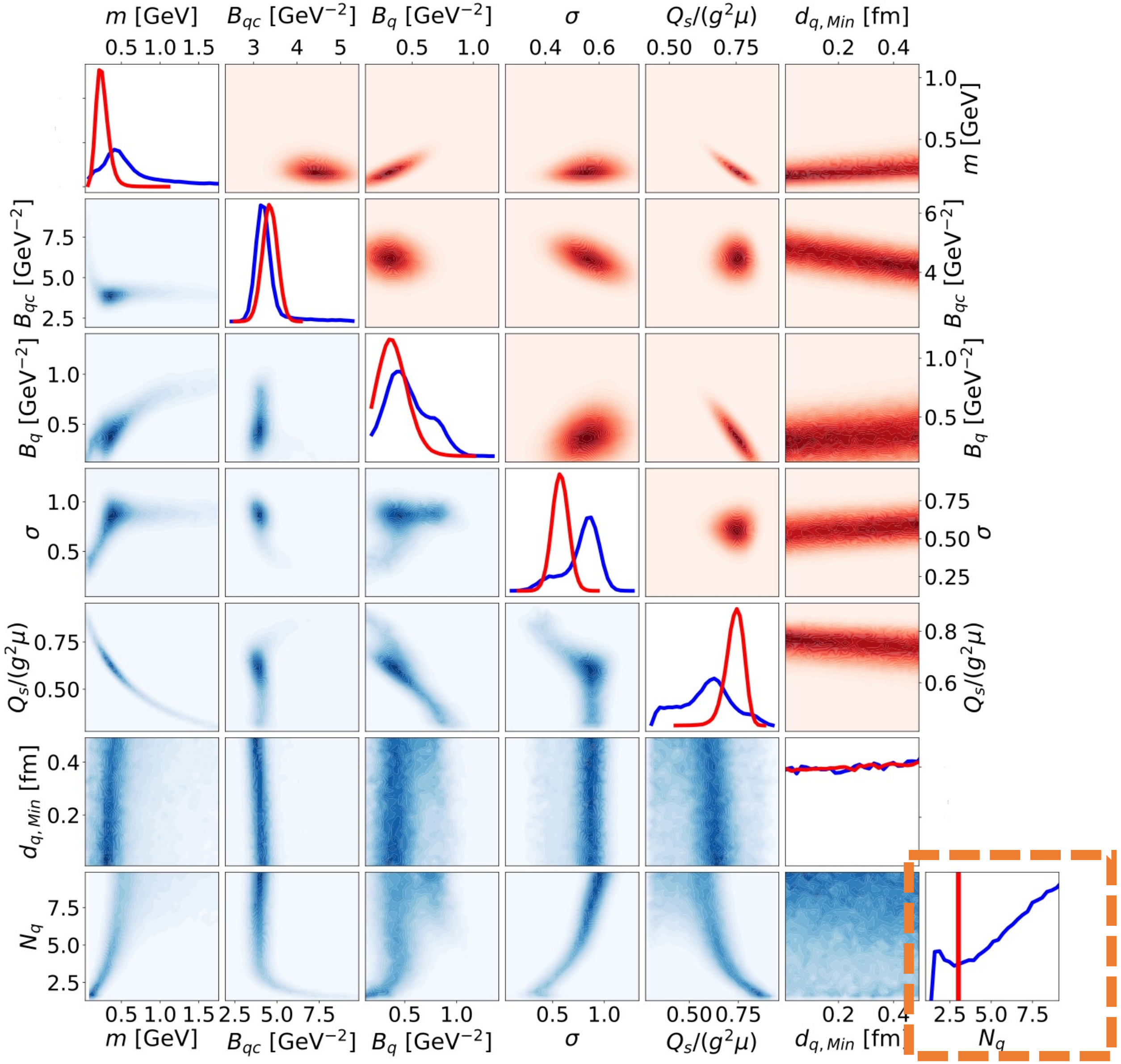

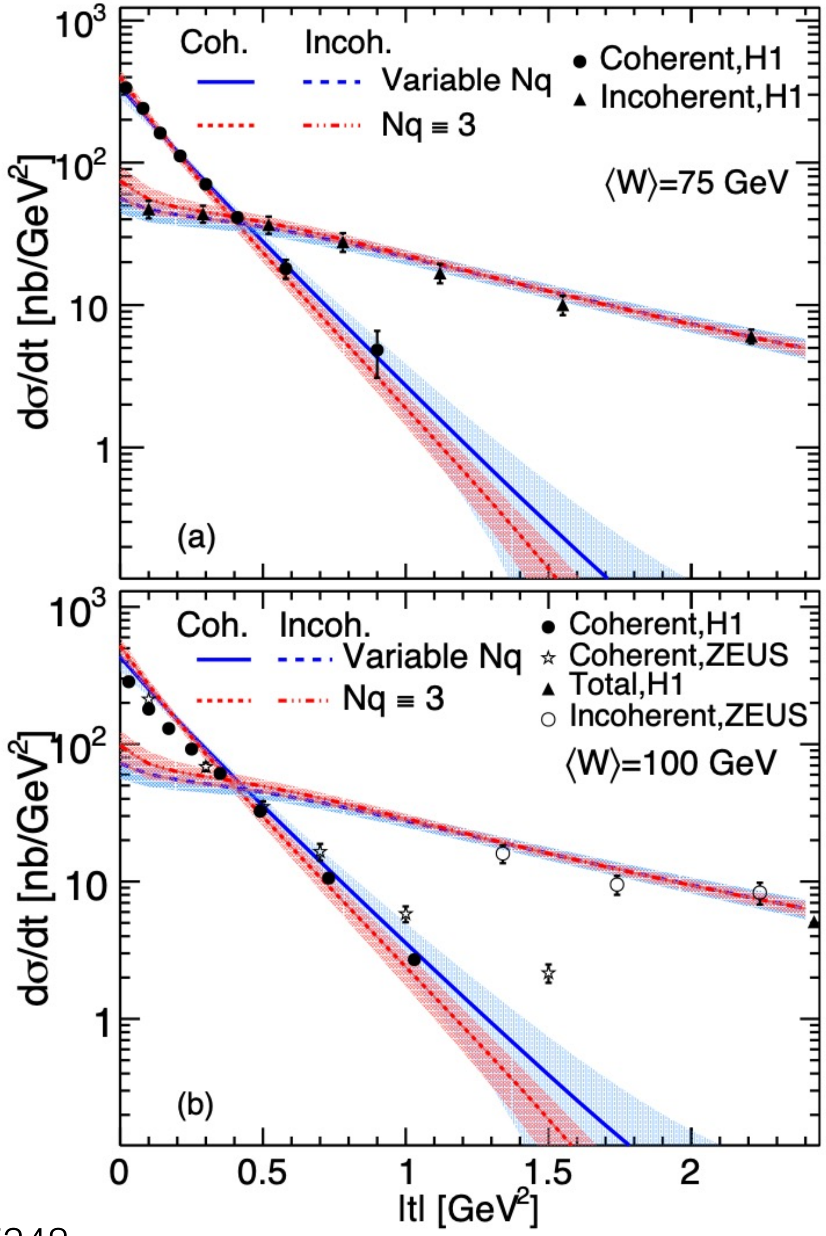

H.Mantysaari, B.Schenke, C. Shen and W. Zhao, Phys. Lett. B 833 (2022), 137348.

Connecting to Relativistic Nuclear Collisions

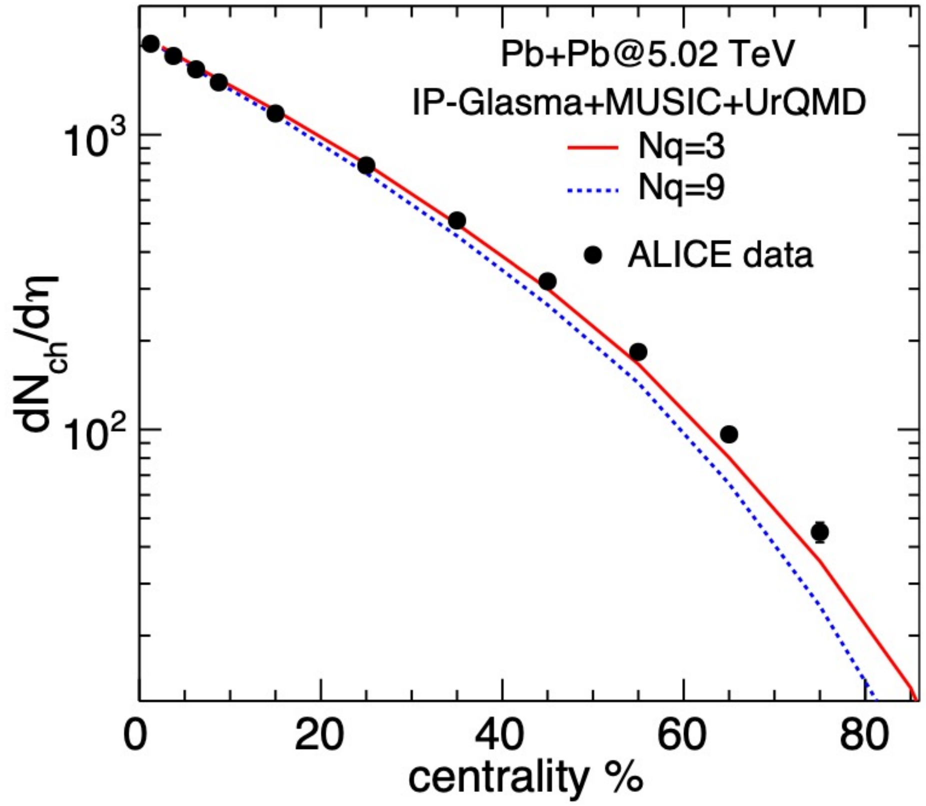

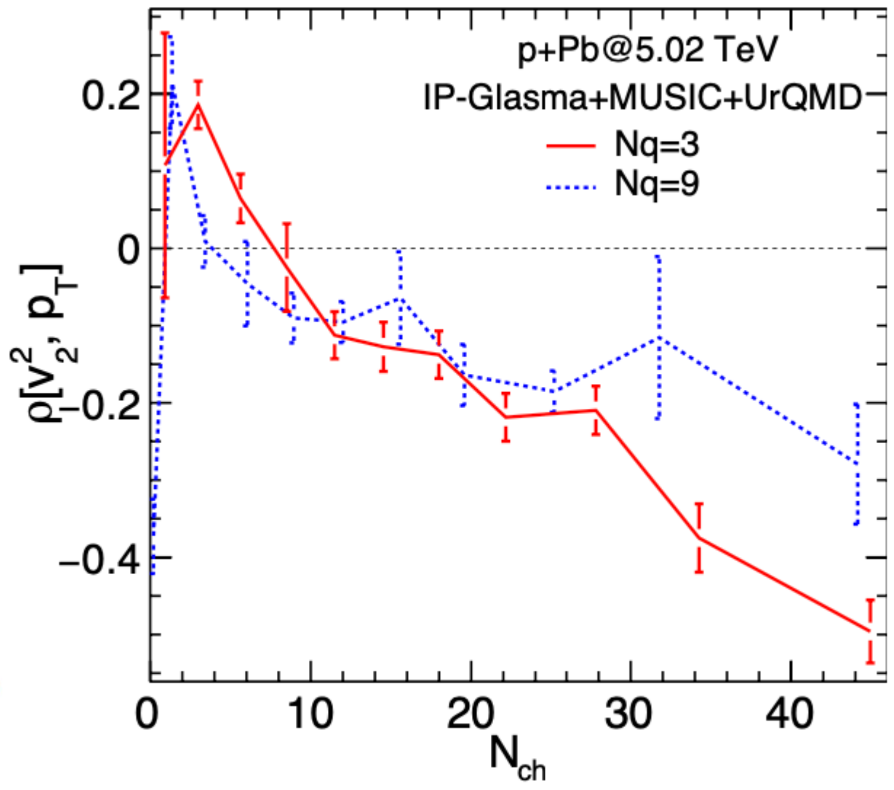

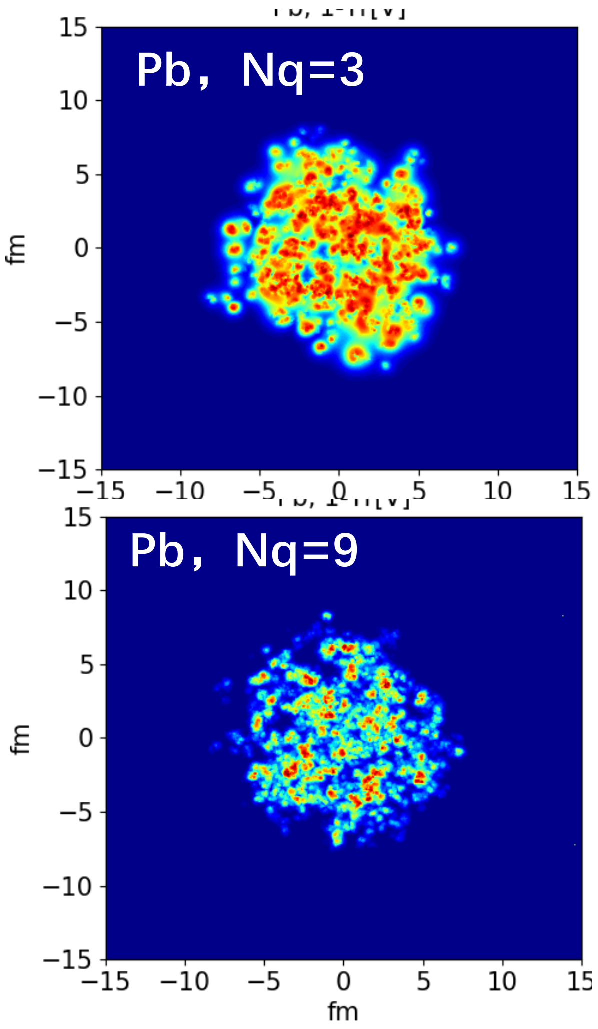

- Pb+Pb $dN_{ch}/d\eta$ data favors the small Nq case.
- $v_2 - p_T$ correlator in p+Pb is a promising observable.

H.Mantysaari, B.Schenke, C. Shen and W. Zhao, Phys. Lett. B 833 (2022), 137348.
H.Mantysaari, B.Schenke, C. Shen and W. Zhao, [arXiv:2208.00396 [hep-ph]].

eU cross section for ρ production

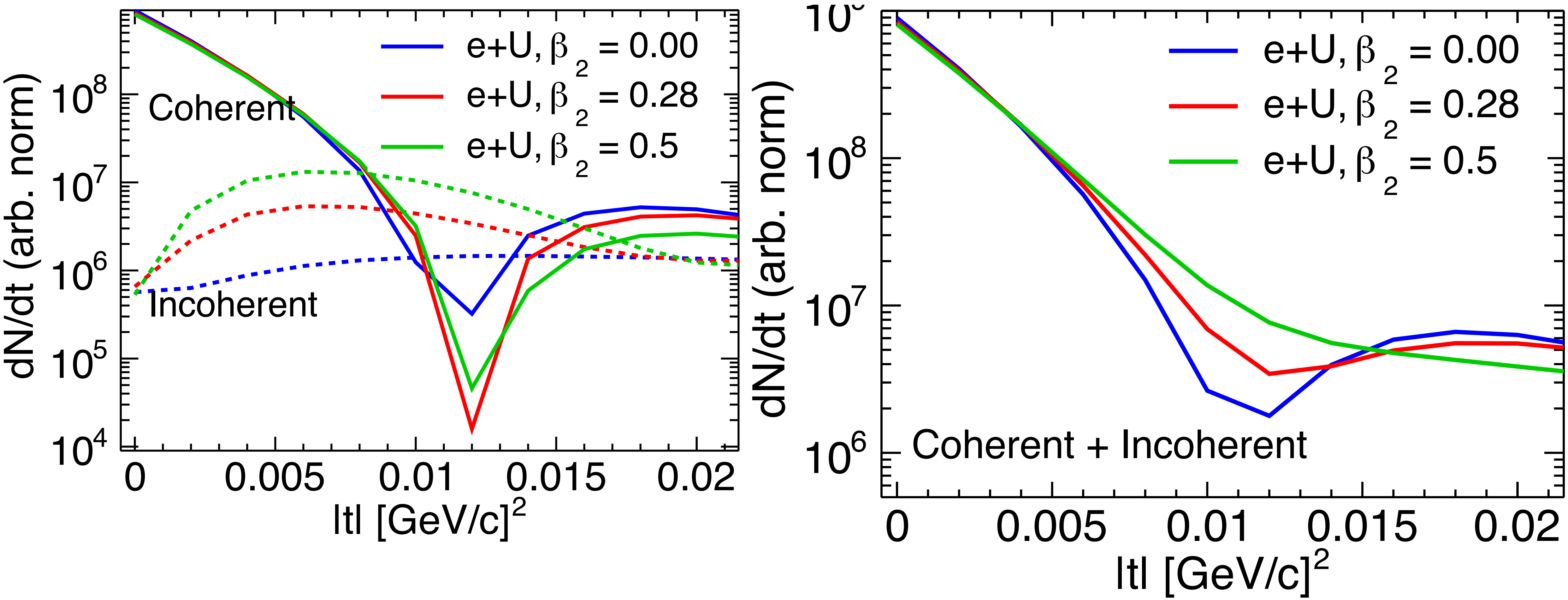

H.Mantysaari, B.Schenke, C. Shen and W. Zhao, Phys. Lett. B 833 (2022), 137348.

Bmin distribution in UPCs

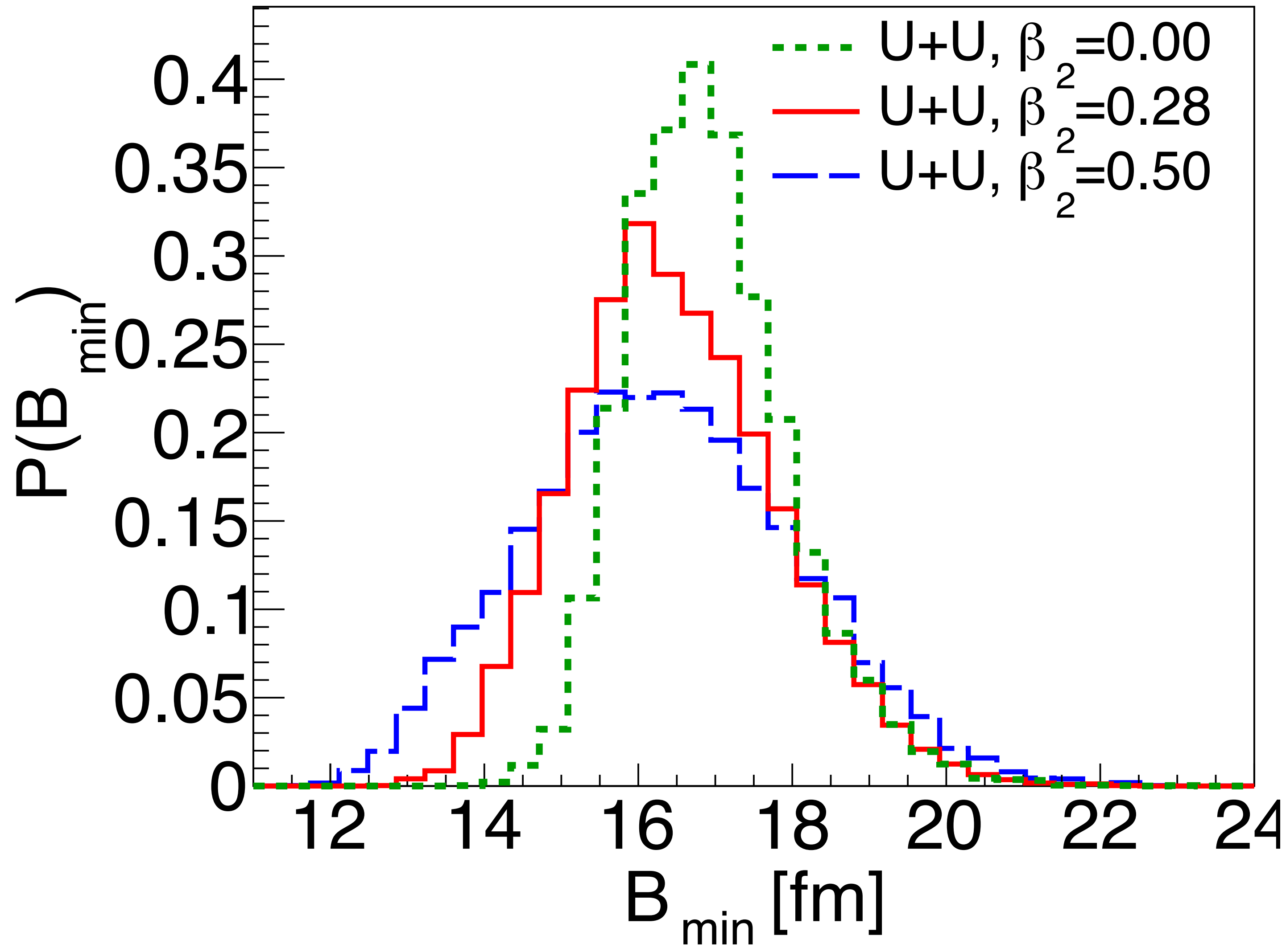

H.Mantysaari, B.Schenke, C. Shen and W. Zhao, Phys. Lett. B 833 (2022), 137348.

Proton geometry fluctuations

- Proton's event-by-event fluctuating density profile:

$$T_p(\mathbf{b}_\perp) = \frac{1}{N_q}\sum_{i=1}^{N_q} p_i T_q(\mathbf{b}_\perp - \mathbf{b}_{\perp,i}), \quad P(\ln p_i) = \frac{1}{\sqrt{2\pi}\sigma}\exp\left[-\frac{\ln^2 p_i}{2\sigma^2}\right].$$

- The density profile of each spot is:

$$T_q(\vec{b}) = \frac{1}{2\pi B_q} e^{-b^2/(2B_q)}$$

- The spot positions $\overrightarrow{b_i}$ are sampled from:

$$P(b_i) = \frac{1}{2\pi B_{qc}} e^{-b_i^2/(2B_{qc})}$$

Schenke , etc.all. PhysRevLett.108.252301 , PhysRevC.86.034908, Mäntysaari, Schenke, 1603.04349;

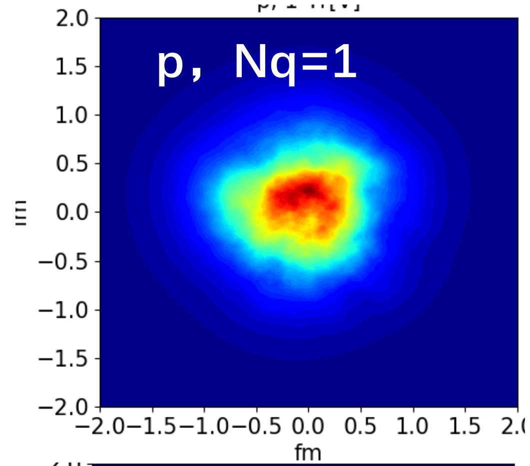

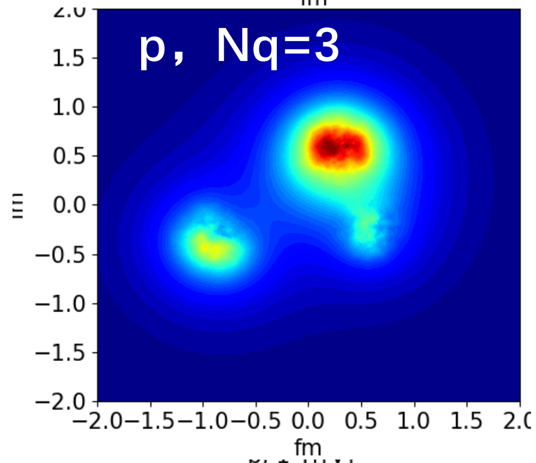

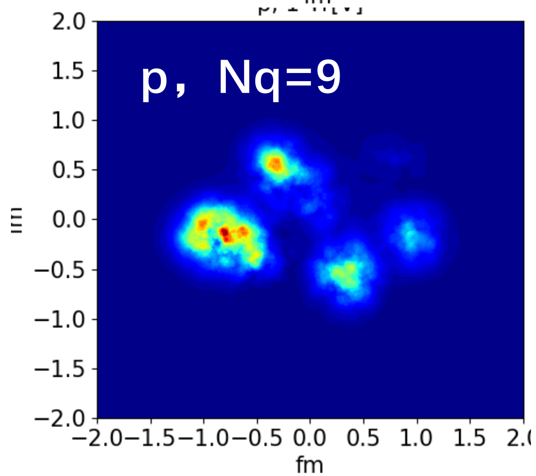

Double-slit interference in UPCs

$$\frac{\mathrm{d}\sigma^{\rho\to\pi^+\pi^-}}{\mathrm{d}^2\mathbf{P}_\perp \mathrm{d}q_\perp \mathrm{d}y_1 \mathrm{d}y_2} =$$

$$\frac{1}{2(2\pi)^3}\frac{P_\perp^2}{(Q^2-M_V^2)^2+M_V^2\Gamma^2}f_{\rho\pi\pi}^2\left\{\int \mathrm{d}\phi_{\mathbf{q}_\perp} B_\perp \mathrm{d}B_\perp \langle \mathcal{M}^i(y,\mathbf{q}_\perp,\mathbf{B}_\perp)\mathcal{M}^{\dagger,j}(y,\mathbf{q}_\perp,\mathbf{B}_\perp)\rangle_\Omega P_\perp^i P_\perp^j \Theta(|\mathbf{B}_\perp|-B_{\mathrm{min},\Omega})\right\}$$

- The amplitude:

$$\mathcal{M}^i(x_1,x_2,\mathbf{q}_\perp,\mathbf{B}_\perp) = \int \mathrm{d}^2\mathbf{b}_\perp e^{-i\mathbf{q}_\perp\cdot\mathbf{b}_\perp}\left[\widetilde{A}(\mathbf{b}_\perp)_{A_1,x_1}\widetilde{\mathcal{F}}^i_{A_2}(x_2,\mathbf{b}_\perp-\mathbf{B}_\perp)+\widetilde{A}(\mathbf{b}_\perp)_{A_2,x_2}\widetilde{\mathcal{F}}^i_{A_1}(x_1,\mathbf{b}_\perp+\mathbf{B}_\perp)e^{-i\mathbf{q}_\perp\cdot\mathbf{B}_\perp}\right],$$

$$\mathcal{A}^{\gamma^* p\to Vp} \sim \int \mathrm{d}^2b\,\mathrm{d}z\,\mathrm{d}^2r\,\Psi^{\gamma*}\Psi^V(r,z,Q^2)\mathbf{e}^{-i\mathbf{b}\cdot\mathbf{\Delta}}N(r,x,b)$$

$\widetilde{\mathcal{F}}^j_A($

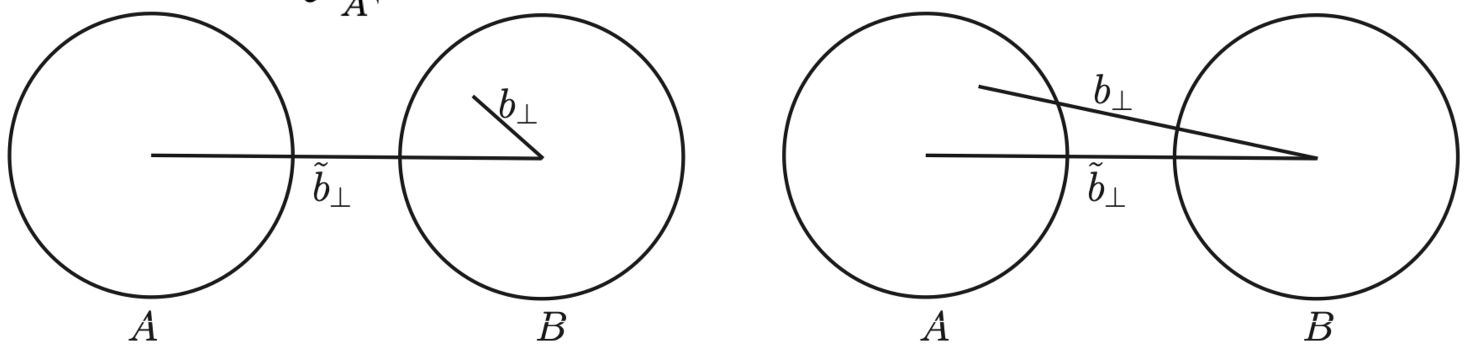

H.Mantysaari, F. Salazar, B.Schenke, C. Shen and W. Zhao, in preparation.
H. Xing, C. Zhang, J. Zhou and Y. J. Zhou, JHEP 10(2020), 064.

Probing ^{20}Ne and ^{16}O

^{20}Ne

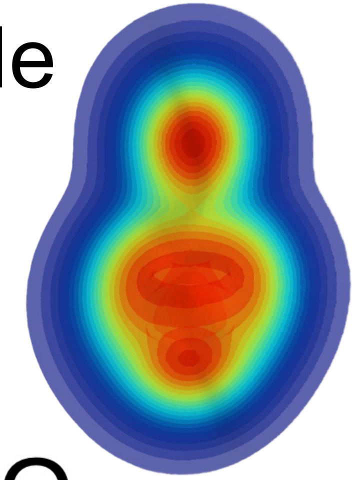

^{16}O

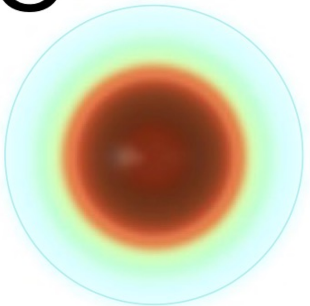

Nucleon density distribution is taken from G. Giacalone.

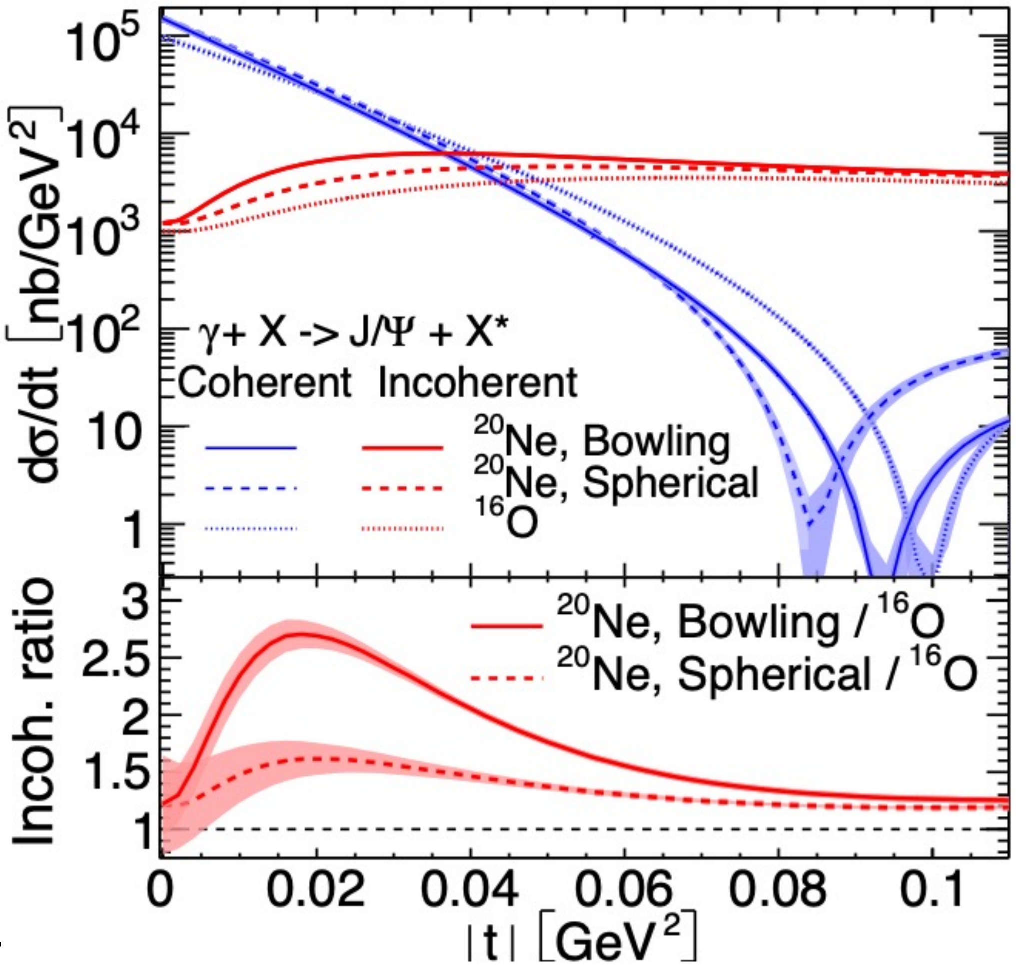

- Incoherent cross section at small |t| captures the deformation of the ^{20}Ne.
- Significant difference between ^{20}Ne and ^{16}O diffractive cross sections is observed.

H.Mantysaari, B.Schenke, C. Shen and W. Zhao, [arXiv:2303.04866] (accepted by PRL).

JIMWLK evolution to smaller xp

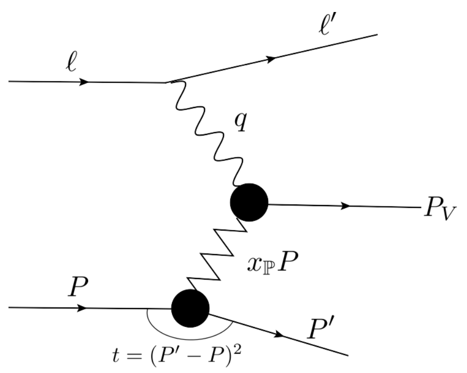

$$x_{\mathbb{P}} \equiv \frac{(P - P') \cdot q}{P \cdot q}$$

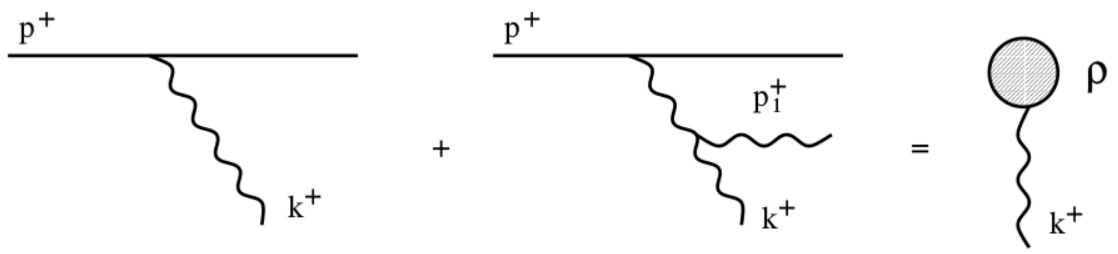

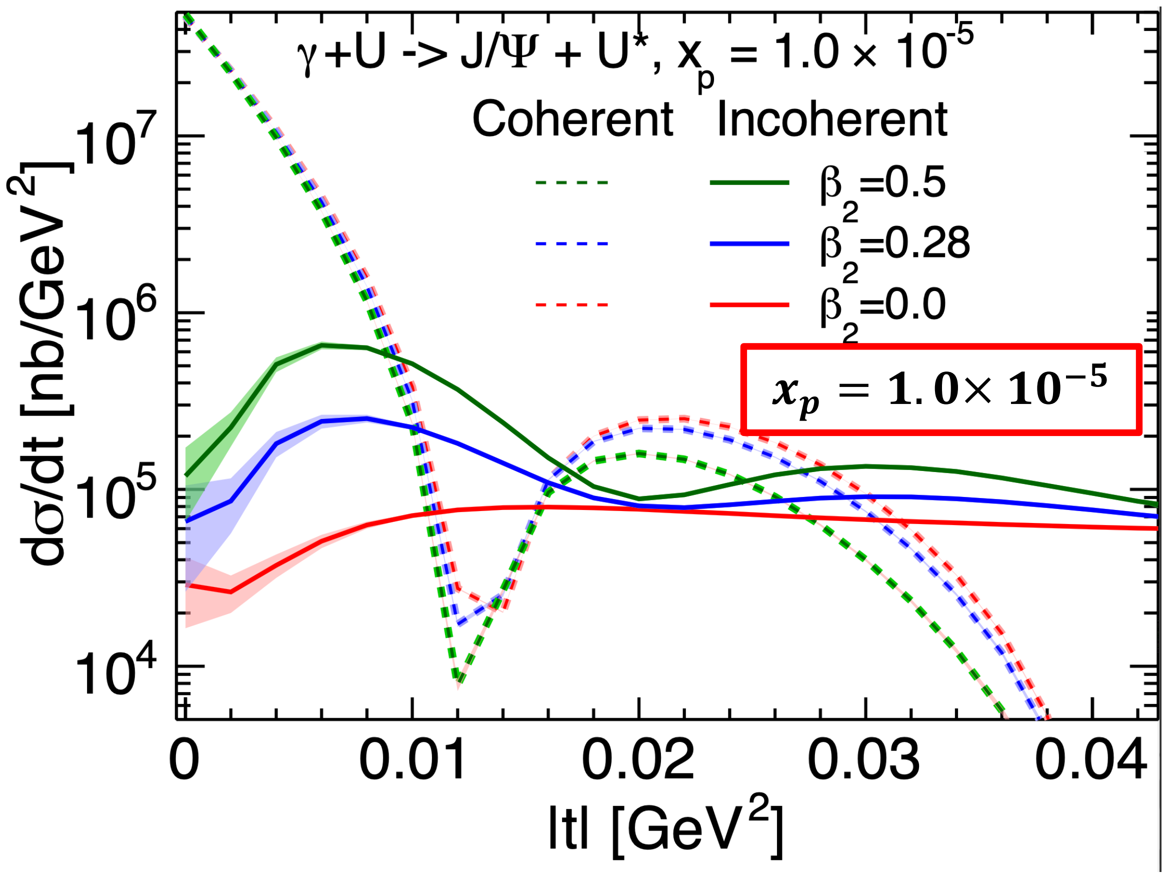

JIMWLK evolution:

absorb quantum fluctuations at intermediate x range as the color sources of smaller x.

- JIMWLK evolution doesn't wash out this effects.

H.Mantysaari, B.Schenke, C. Shen and W. Zhao [arXiv:2303.04866] (accepted by PRL).

H.Mantysaari, B.Schenke PRD, 98, 034013.

T. Lappi and H. Mantysaari, EPJC 73, 2307 (2013).

Yuri V. Kovchegov, QUANTUM CHROMODYNAMICS A T HIGH ENERGY

Probing protons at different resolutions

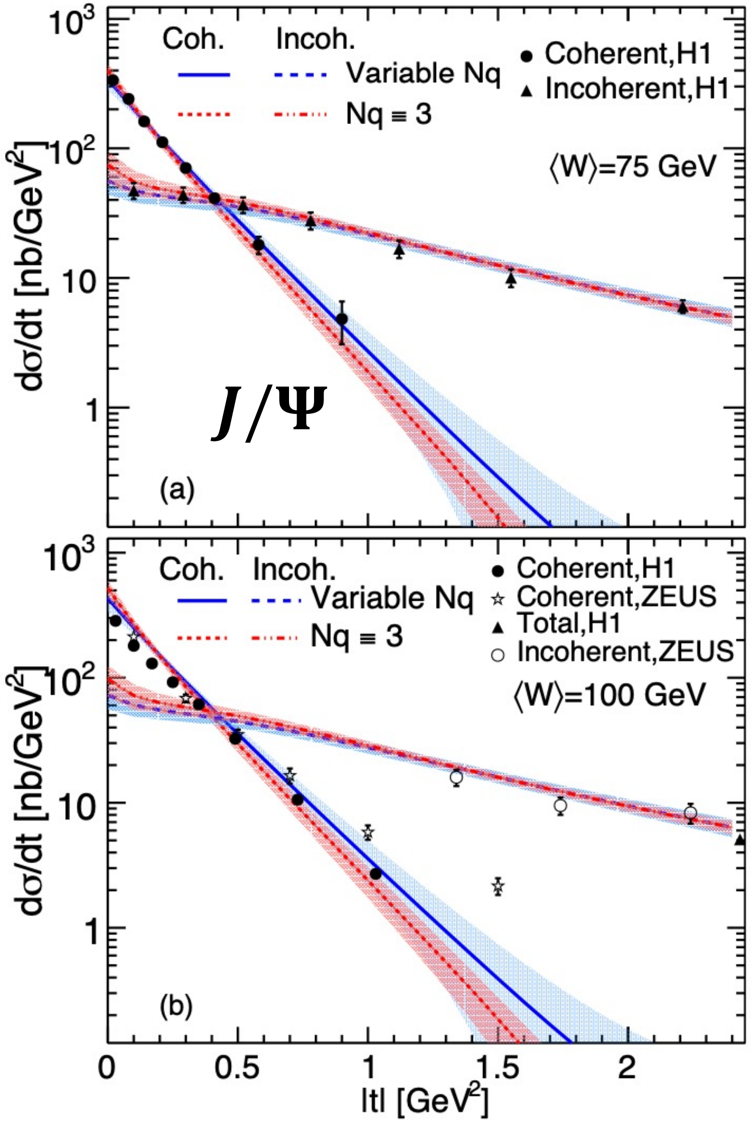

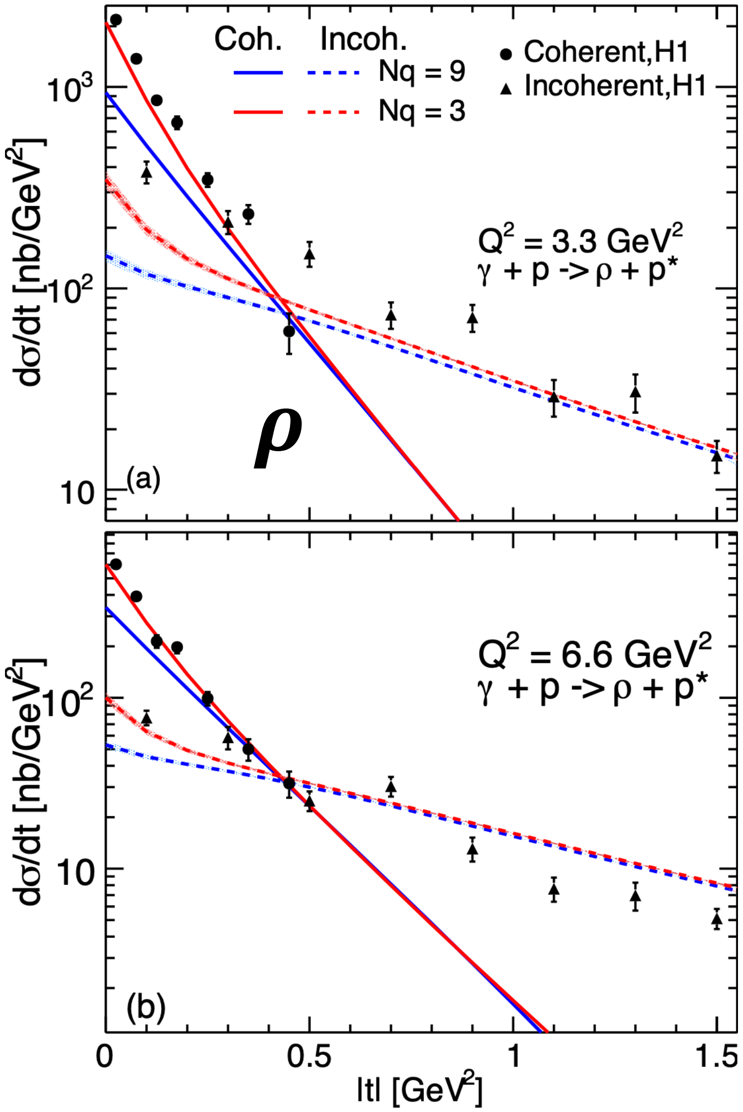

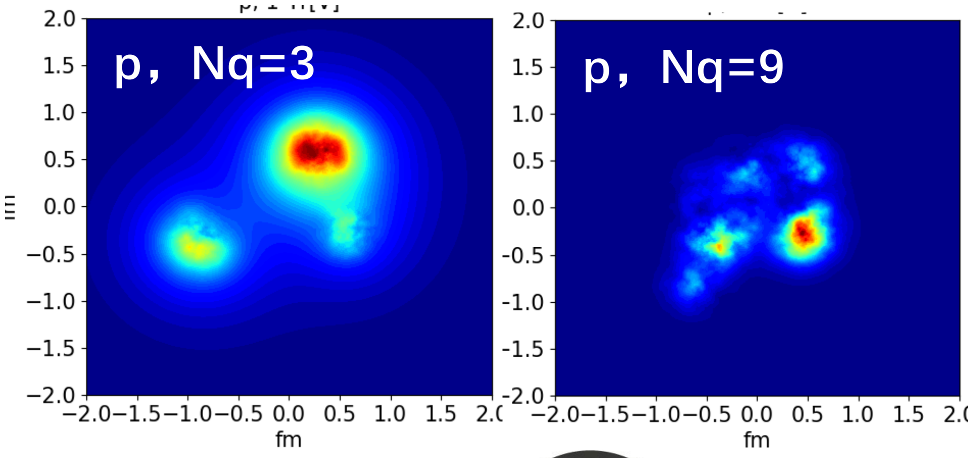

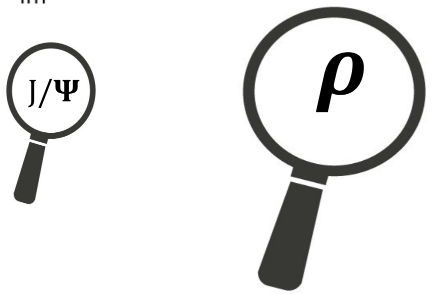

- The ρ mesons probe proton fluctuations at large length scales.
- Large differences observed for ρ productions between Nq=3 and Nq=9 MAPs.

H. Mantysaari, B.Schenke, C. Shen and W. Zhao, Phys. Lett. B 833 (2022), 137348, and in progress.

Model parameters and the Exp. Data (γ^* + p $\rightarrow$ J/ψ + p*)

Parameterize proton shape (T_p)

- Number of hot spots N_q
- Proton size B_{qc}
- Hot spot size B_q
- Hot spot density fluctuations σ
- Min. distance between hot spots $d_{q,min}$
- Overall color charge density: $Qs(x)/g^2\mu$
- Infrared regulator m

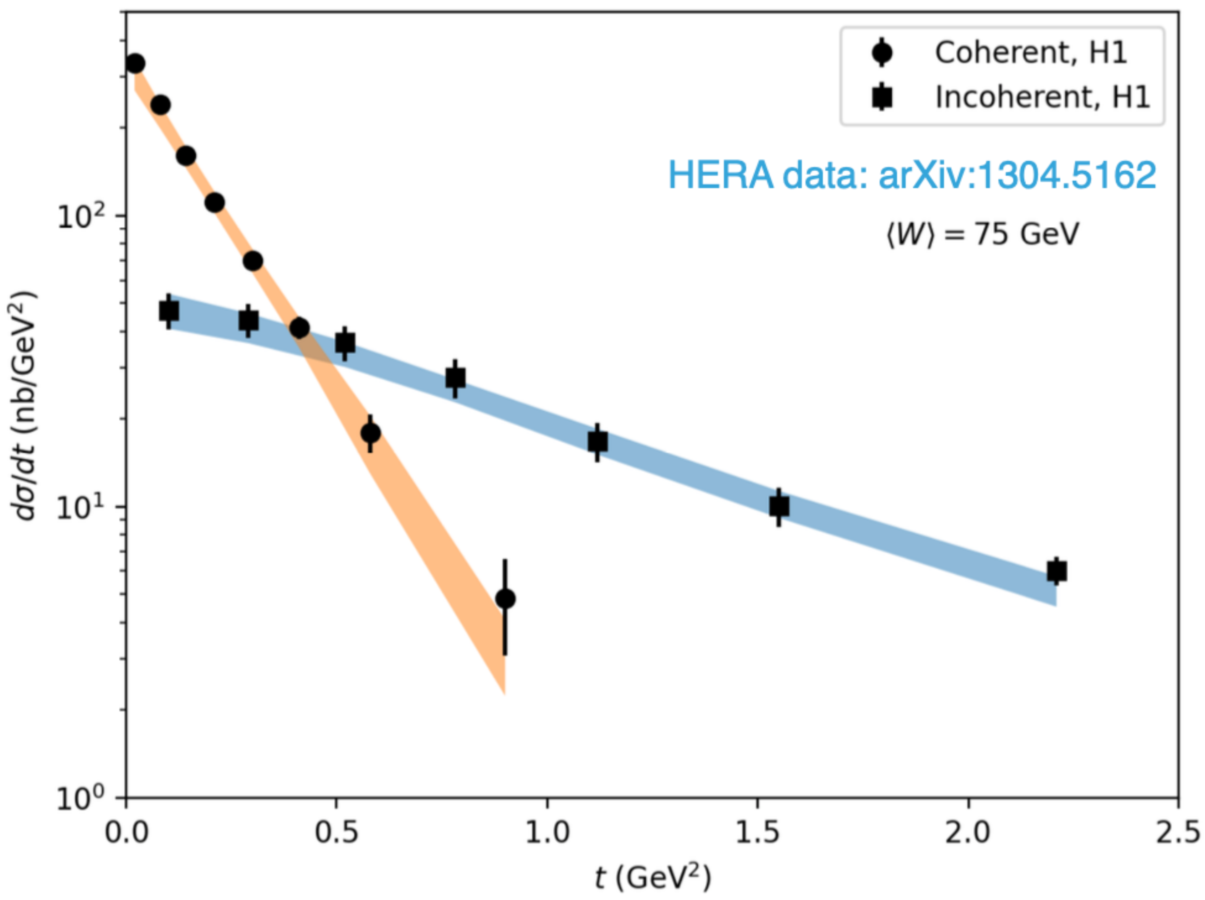

- 7D parameter space; generated 1000 training points for the model emulator

H.Mantysaari, B.Schenke, C. Shen and W. Zhao, Phys. Lett. B 833 (2022), 137348.

JIMWLK evolution to smaller xp

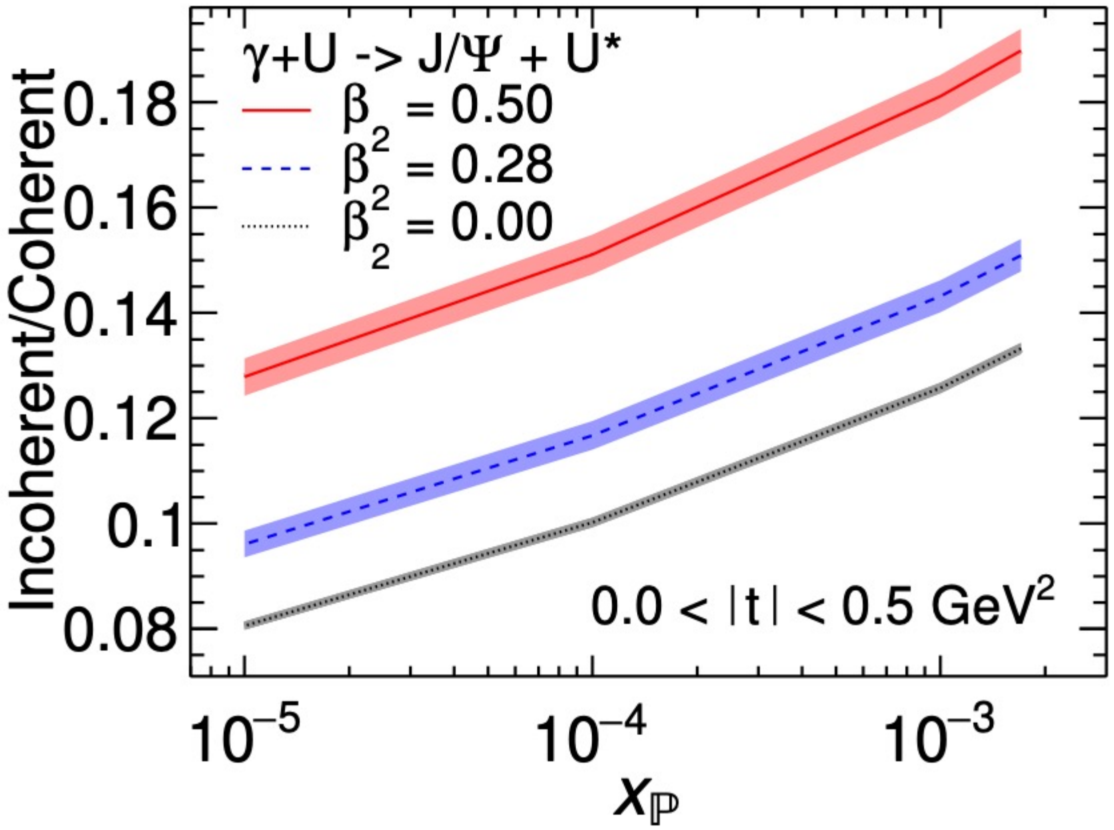

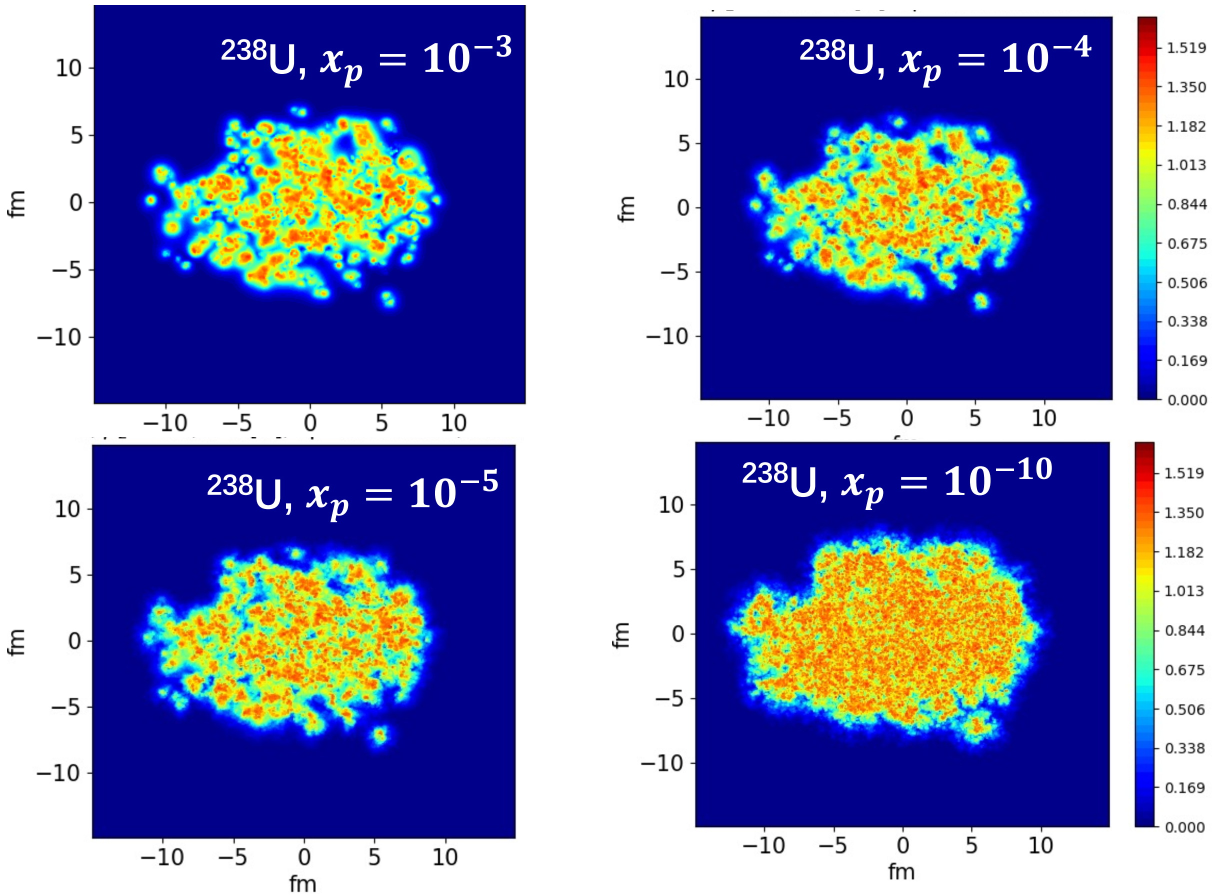

- Incoherent-to-coherent ratio effectively suppresses model uncertainties from wave functions.
- At smaller x_p, nucleon is smoother, reduces the fluctuations, decreases Incoherent-to-coherent ratio.
- JIMWLK evolution doesn't wash out difference between different β_2 (β_2 controls overall shape).

H.Mantysaari, B.Schenke, C. Shen and W. Zhao, [arXiv:2303.04866].
H.Mantysaari, B.Schenke PRD, 98, 034013.

Degeneracy in the number of hot spots

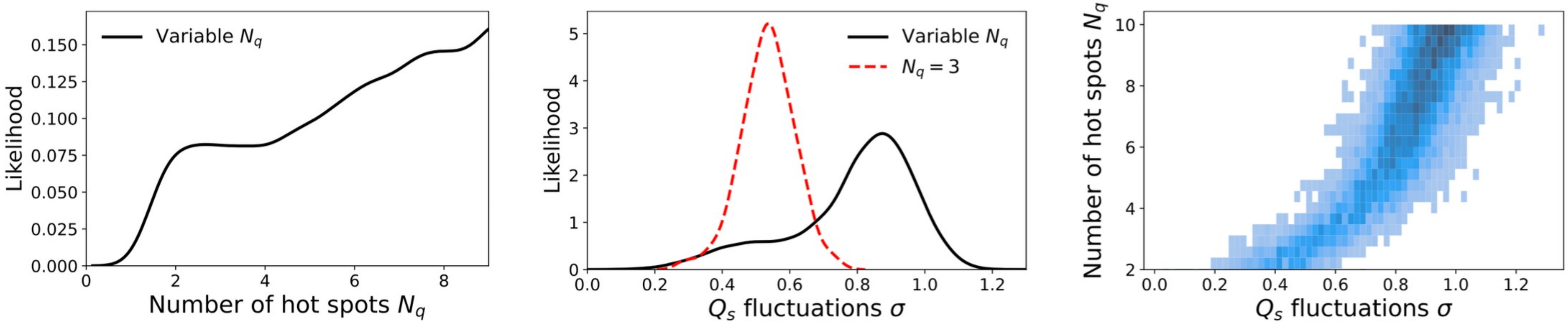

- The likelihood of number of hot spots Nq increases monotonously.
- Large Nq partially compensated by large Qs fluctuations, $\sigma \propto \sqrt{N_q}$, "number of effective hot spots" < Nq
- **Proton's event-by-event fluctuating density profile:**

$$T_p(\mathbf{b}_\perp) = \frac{1}{N_q}\sum_{i=1}^{N_q} p_i T_q(\mathbf{b}_\perp - \mathbf{b}_{\perp,i}), \quad P\left(\ln p_i\right) = \frac{1}{\sqrt{2\pi}\sigma}\exp\left[-\frac{\ln^2 p_i}{2\sigma^2}\right].$$

H. Mantysaari, B.Schenke, C. Shen and W. Zhao, Phys. Lett. B 833 (2022), 137348.
H. Mantysaari, B.Schenke, C. Shen and W. Zhao, [arXiv:2208.00396 [hep-ph]].

MAP of fixed Nq=3 and Nq=9

Parameter	Description	$N_q = 9$	$N_q = 3$
m [GeV]	Infrared regulator	0.780	0.246
B_{qc} [GeV^{-2}]	Proton size	3.98	4.45
B_q [GeV^{-2}]	Hot spot size	0.594	0.346
σ	Magnitude of Q_s fluctuations	0.932	0.563
$Q_s/(g^2\mu)$	$Q_s \Rightarrow$ color charge density	0.492	0.747
$d_{q,\mathrm{Min}}$ [fm]	Min hot spot distance	0.265	0.254
N_q	Number of hot spots	3	9
S	Hydro normalization	0.1135	0.235

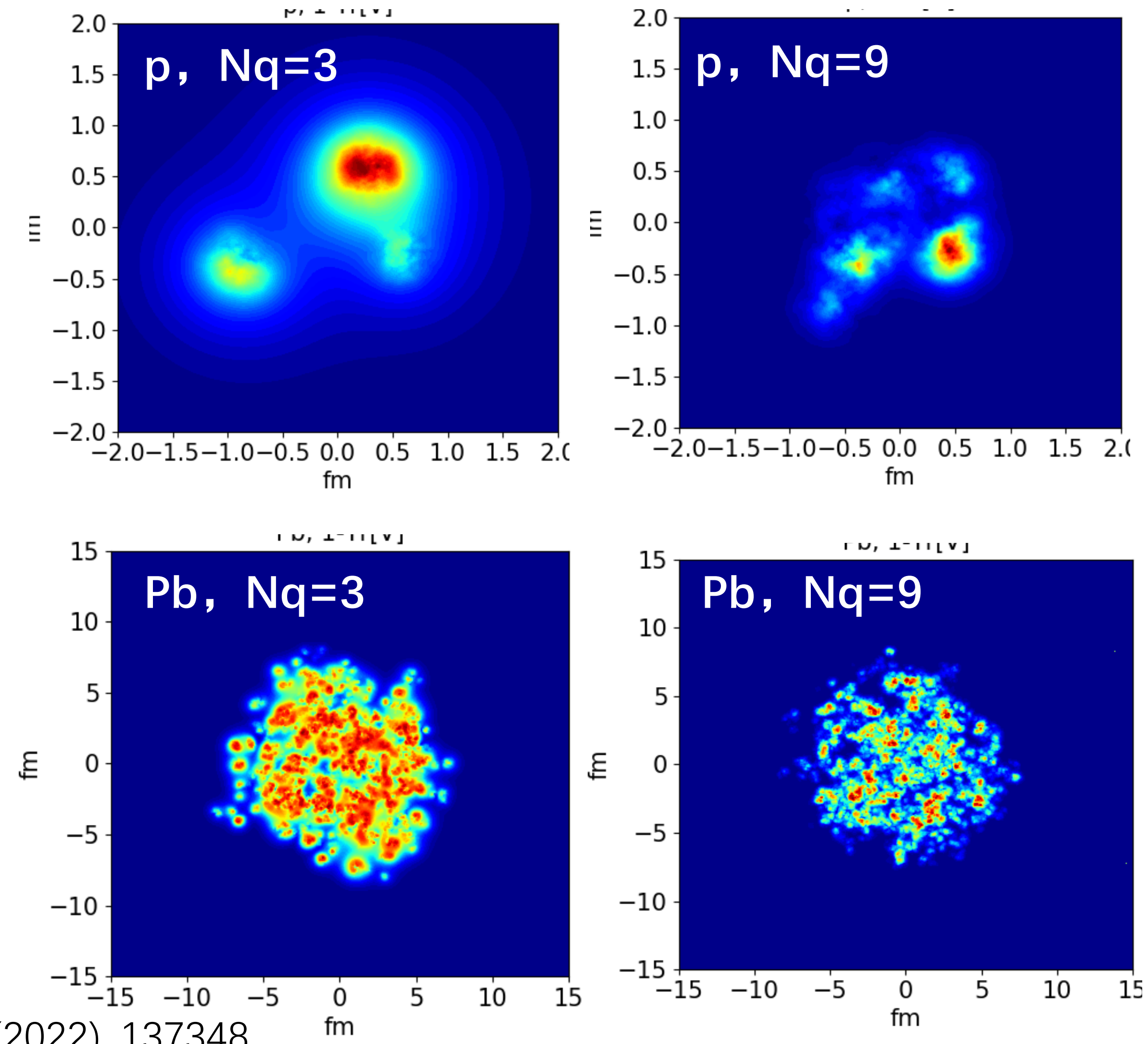

- The Nq=3 and Nq=9 have the different configurations at large length scales.
- “See” them by the different probes.

H. Mantysaari, B.Schenke, C. Shen and W. Zhao, Phys. Lett. B 833 (2022), 137348.
H. Mantysaari, B.Schenke, C. Shen and W. Zhao, [arXiv:2208.00396 [hep-ph]].

Proton & hotspot sizes at high energy

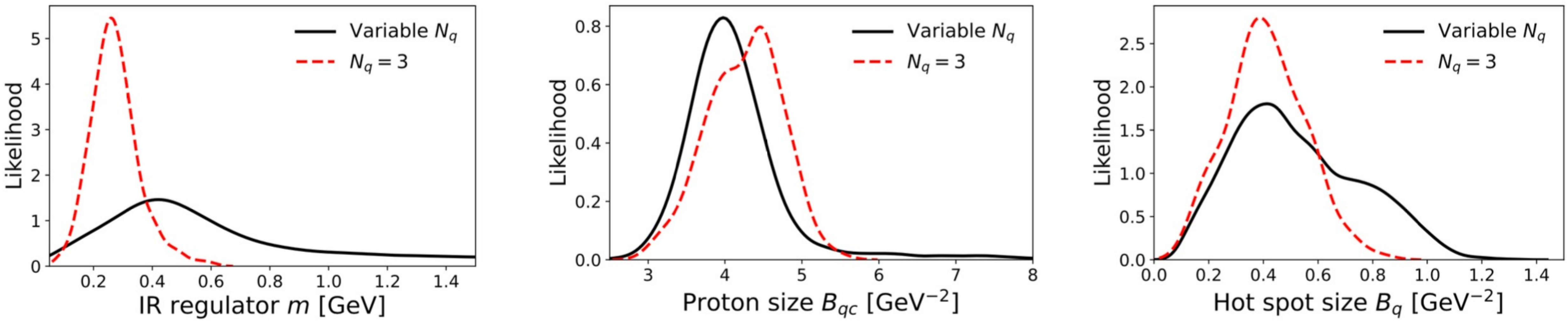

- Some parameters are well constrained .
- The 2D RMS proton radius $R_{rms} = \sqrt{2(B_{qc} + B_q)} \sim$ 0.6 fm, which is consistent with the results in heavy-ion collisions.

H.Mantysaari, B.Schenke, C. Shen and W. Zhao, Phys. Lett. B 833 (2022), 137348.
H.Mantysaari, B.Schenke, C. Shen and W. Zhao, [arXiv:2208.00396 [hep-ph]].
G. Giacalone, B. Schenke and C. Shen, Phys. Rev. Lett. 128, 042301 (2022)

Dipole-target scattering amplitude (CGC)

- The dipole amplitude N can be calculated from Wilson line V(x)

$$N\left(\mathbf{b}=\frac{\mathbf{x}+\mathbf{y}}{2},\mathbf{r}=\mathbf{x}-\mathbf{y},x_{\mathbb{P}}\right)=1-\frac{1}{N_c}\mathrm{Tr}\left(V(\mathbf{x})V^{\dagger}(\mathbf{y})\right) \quad V(\mathbf{x})=P\exp\left(-ig\int dx^{-}\frac{\rho(x^{-},\mathbf{x})}{\boldsymbol{\nabla}^2+m^2}\right)$$

- Using MV model for Gaussian distribution of color charge ρ:

$$\langle\rho^a(\mathbf{b}_\perp)\rho^b(\mathbf{x}_\perp)\rangle=g^2\mu^2(x,\mathbf{b}_\perp)\delta^{ab}\delta^{(2)}(\mathbf{b}_\perp-\mathbf{x}_\perp)$$

Q_s: saturation scale, $Q_s/g^2\mu$ is a free parameter, Q_s is determined from IP-Sat parametrization.

- Or, equivalently, factorize $\mu(x,\mathbf{b}_\perp)\sim T(\mathbf{b}_\perp)\mu(x)$

$\boxed{\text{N(r, x, b) accesses to the spatial structure of the target } (T_{p/A}).}$

Schenke , etc.al. PhysRevLett.108.252301 , PhysRevC.86.034908, Mäntysaari, Schenke, 1603.04349;

Diffractive vector meson production

High energy factorization:

1. $\gamma^* \to q\bar{q}$ splitting,
   wave function $\Psi^\gamma(r, Q^2, z)$
2. $q\bar{q}$ dipole scatters elastically
3. $q\bar{q} \to J/\Psi$, wave function $\Psi^V(r, Q^2, z)$

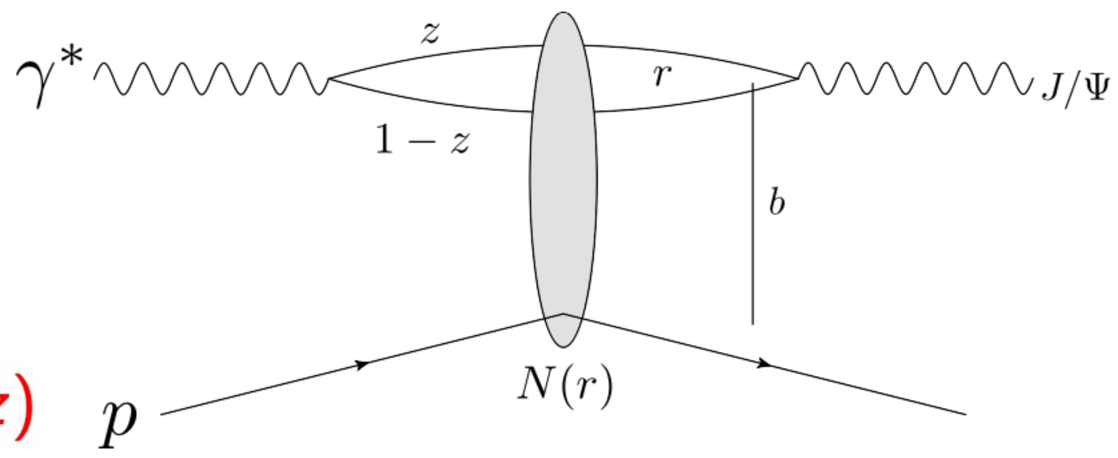

Diffractive scattering amplitude

$$\mathcal{A}^{\gamma^* p \to Vp} \sim \int \mathrm{d}^2 b \mathrm{d}z \mathrm{d}^2 r \Psi^{\gamma *} \Psi^V(r, z, Q^2) \mathbf{e}^{-i\mathbf{b}\cdot\boldsymbol{\Delta}} N(r, x, b)$$

Impact parameter, b, is the Fourier conjugate of the momentum transfer, $\Delta \approx \sqrt{-t}$

N(r, x, b) dipole-target scattering amplitude.

Miettinen, Pumplin, PRD 18, 1978; Caldwell, Kowalski, 0909.1254; Mäntysaari, Schenke, 1603.04349; Mäntysaari, 2001.10705

Dipole-target scattering amplitude (IP-Sat)

$N(\mathbf{r}_T, \mathbf{b}_T, x) = 1 - \exp\left(-\mathbf{r}_T{}^2 F(\mathbf{r}_T, x) T_p(\mathbf{b}_T)\right)$ **accesses to the spatial structure ($\boldsymbol{T_{p/A}}$)**

$F(\mathbf{r}_T, x) = \dfrac{\pi^2}{2N_c} \alpha_s(\mu^2) x g(x, \mu^2)$. $xg(x, \mu^2)$, gluon density at x and scale μ^2 $(\mu^2 \sim \mu_0^2 + 1/r_T^2)$.

$$\mathcal{A}^{\gamma^* p \to Vp} \sim \int \mathrm{d}^2 b \mathrm{d}z \mathrm{d}^2 r \Psi^{\gamma *} \Psi^{V}(r, z, Q^2) \mathbf{e}^{-\mathbf{i}\mathbf{b}\cdot\mathbf{\Delta}} N(r, x, b)$$

- Diffractive scattering amplitude is roughly proportional to Fourier transform of the spatial structure function of target (Tp/A).

Miettinen, Pumplin, PRD 18, 1978; Caldwell, Kowalski, 0909.1254; Mäntysaari, Schenke, 1603.04349; Mäntysaari, 2001.10705

Probing isobar, Ru/Zr

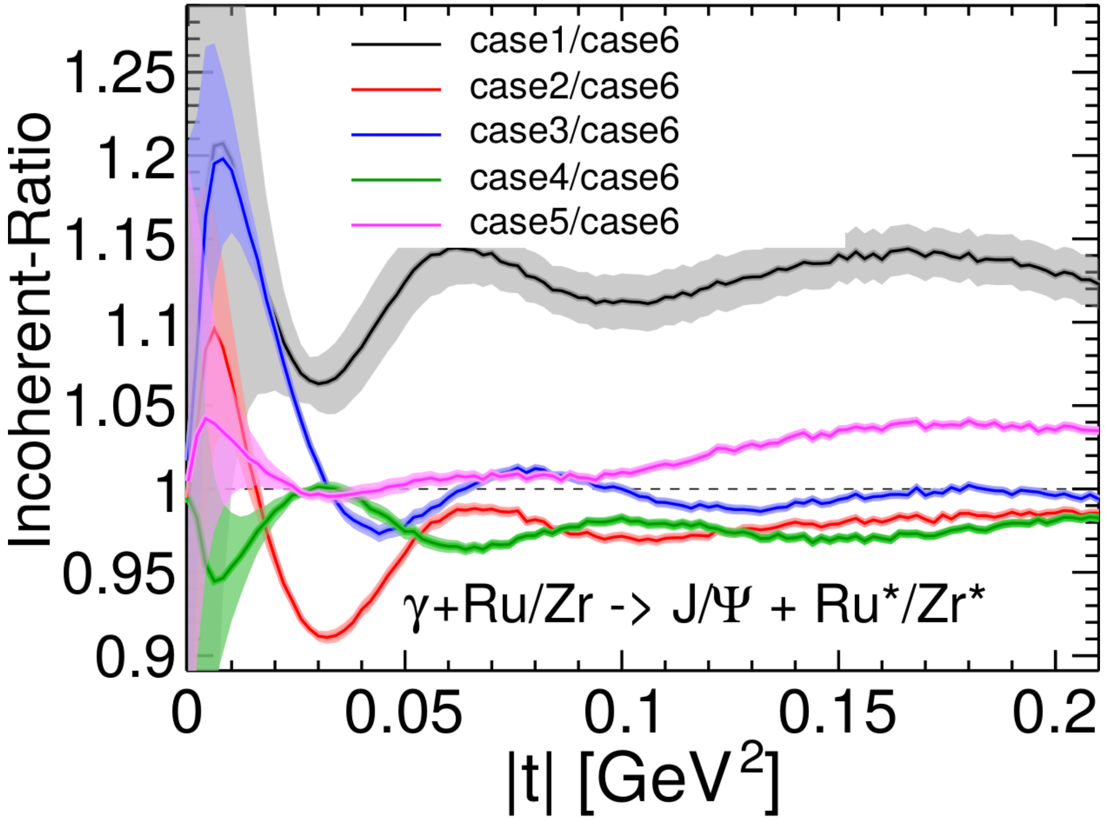

- Differences of incoherent J/Ψ productions cross section between case2 -- case6 are within 5%.
- The difference between case1 and others mainly comes from dmin.

H.Mantysaari, B.Schenke, C. Shen and W. Zhao, in progress.